



## **Robust Energy Transition Pathways for Global Warming Targets**

**Claire NICOLAS  
Stéphane TCHUNG-MING  
Olivier BAHN  
Erick DELAGE**

*September 2016*

**Les cahiers de l'économie - n° 108**

**Série Recherche**

[claire.m.nicolas@gmail.com](mailto:claire.m.nicolas@gmail.com)  
[stephane.tchungming@gmail.com](mailto:stephane.tchungming@gmail.com)

La collection "Les cahiers de l'économie" a pour objectif de présenter des travaux réalisés à IFP Énergies Nouvelles et à IFP School, travaux de recherche ou notes de synthèse en économie, finance et gestion. La forme peut être encore provisoire, afin de susciter des échanges de points de vue sur les sujets abordés. Les opinions émises dans les textes publiés dans cette collection doivent être considérées comme propres à leurs auteurs et ne reflètent pas nécessairement le point de vue d' IFP Énergies Nouvelles ou d' IFP School.

Pour toute information sur le contenu, prière de contacter directement l'auteur.  
Pour toute information complémentaire, prière de contacter le Centre Économie et Gestion: Tél +33 1 47 52 72 27

*The views expressed in this paper are those of the authors and do not imply endorsement by the IFP Energies Nouvelles or the IFP School. Neither these institutions nor the authors accept any liability for loss or damage incurred as a result of the use of or reliance on the content of this publication.*



# Robust Energy Transition Pathways for Global Warming Targets

Claire Nicolas<sup>1,\*</sup>, Stéphane Tchong-Ming<sup>1</sup>, Olivier Bahn<sup>2</sup>, Erick Delage<sup>2</sup>

<sup>1</sup>*IFP Energies nouvelles, 1-4 avenue de Bois-Préau, 92852 Rueil-Malmaison, France*

<sup>2</sup>*GERAD and Department of Decision Sciences, HEC Montréal, 3000, chemin de la Côte-Sainte-Catherine, Montréal (Québec), Canada H3T 2A7*

---

## Abstract

In this paper, we study how uncertainties weighing on the climate system impact the optimal technological pathways the world energy system should take to comply with stringent mitigation objectives. We use the TIAM-World model that relies on the TIMES modelling approach. Its climate module is inspired by the DICE model. Using robust optimization techniques, we assess the impact of the climate system parameter uncertainty on energy transition pathways under various climate constraints. Unlike other studies we consider all the climate system parameters which is of primary importance since: (i) parameters and outcomes of climate models are all inherently uncertain (parametric uncertainty); and (ii) the simplified models at stake summarize phenomena that are by nature complex and non linear in a few, sometimes linear, equations so that structural uncertainty is also a major issue. The use of robust optimization allows us to identify economic energy transition pathways under climate constraints for which the outcome scenarios remain relevant for any realization of the climate parameters. In this sense, transition pathways are made robust. We find that the abatement strategies are quite different between the two temperature targets. The most stringent one is reached by investing massively in carbon removal technologies such as bioenergy with carbon capture and storage (BECCS) which have yields much lower than traditional fossil fuelled technologies.

*Keywords:* Robust optimization; Climate change; Climate modelling

---

---

\*Corresponding author

*Email addresses:* [claire.m.nicolas@gmail.com](mailto:claire.m.nicolas@gmail.com) (Claire Nicolas), [stephane.tchungming@gmail.com](mailto:stephane.tchungming@gmail.com) (Stéphane Tchong-Ming), [olivier.bahn@hec.ca](mailto:olivier.bahn@hec.ca) (Olivier Bahn), [erick.delage@hec.ca](mailto:erick.delage@hec.ca) (Erick Delage)

# 1. Introduction

According to the Intergovernmental Panel on Climate Change (Stocker et al., 2013), anthropogenic greenhouse gas (GHG) emissions, such as carbon dioxide (CO<sub>2</sub>) emissions from the combustion of fossil fuels, play an important role in the warming of the climate system. This global warming and the associated climate changes pose important threats to ecosystems and human societies (IPCC, 2014). To cope with these threats, a possible strategy is to reduce GHG emissions, the so-called mitigation approach<sup>1</sup>. The latter has been put forward by the Paris Agreement (United Nations, 2015) to the United Nations Framework Convention on Climate Change (UNFCCC), which calls for a strong reduction in GHG emissions to limit global temperature rise to “*well below*” 2 °C, with an aim to limit the increase to 1.5 °C.

To design climate mitigation policies, and especially to analyze energy transition pathways ensuring a strong abatement of GHG emissions, one may follow an integrated assessment (IA) approach. The latter typically combines the socio-economic elements that drive GHG emissions with the geophysical and environmental elements that determine climate changes and their impacts. Integrated assessment models (IAMs) are computational tools to perform IA. Examples of such models include: BaHaMa (Bahn et al., 2015), DICE (Nordhaus, 2014), FUND (Anthoff and Tol, 2013), MERGE (Manne et al., 1995), PAGE (Hope, 2006) and TIAM-World (Loulou and Labriet, 2008).

These IAMs operate under different paradigms (e.g., bottom-up or top-down, optimization or simulation, . . .). Furthermore, they specifically vary with respect to the level of modelling details for the mitigation options. At both ends of the spectrum, DICE aggregates (following a top-down philosophy) all mitigation options into a single cost function, whereas TIAM-World offers a very detailed bottom-up representation of the energy sector with thousands of energy technologies following the TIMES paradigm of the International Energy Agency. This large variety of IAMs used, along with our current imperfect knowledge of all the climate change mechanisms, yield sometimes very different climate policy recommendations. For instance, Stern (2007) has advocated using PAGE for immediate actions to abate GHG emissions. While, conversely, Nordhaus (2008), with his DICE model, has reached the conclusion that immediate and massive actions are not necessary.

This lack of robustness across models leads some economists to disregard the use of current IAMs (Pindyck, 2013; Stern, 2013). It is indeed undeniable that the long-term energy-economy-climate outlook provided by current IAMs is clouded with a great degree of uncertainty that may deeply affect the relevance of the policy analyses performed and the validity of the policy recommendations formulated. The source of this uncertainty is multiple (see for instance van Asselt and Rotmans, 2002). Moreover, even small variations in data can impact feasibility or optimality properties of a given solution (Ben-tal and Nemirovski, 2000). It is thus important to make uncertainty a core feature of long-term climate policy analyses using IAMs.

Several approaches have been followed to address uncertainties in IAMs, in particular: deterministic multi-scenario analysis, sensitivity analysis and Monte-Carlo simulations, stochastic programming and stochastic control. These approaches are quite useful but all have drawbacks. Sensitivity analysis and Monte-Carlo simulations make way for the investigation of the impact of particular parameters, but do not provide unambiguous hedging strategies. Deterministic multi-scenario analysis results are also difficult to interpret as models are run in a deterministic way with little possibility to probabilize the scenario occurrence. The stochastic programming drawback is that probability distributions (eventually parameterized) have to be defined over

---

<sup>1</sup>Alternative strategies are adaptation to climate change impacts and the use of geoengineering measures.

the whole tree and that conclusions might be sensitive to the choice of scenario and branching scheme. Moreover, stochastic programming may considerably increase the size of the problem to be solved, leading quickly to excessive computational times. Computational burden also typically limits the use of stochastic control approaches in IAMs.

In this paper, we use robust optimization (RO). Early developments date back to [Soyster \(1973\)](#), who initiated an approach to obtain relevant (feasible) LP solutions although matrix coefficients are inexact. This idea has then been largely explored with different formalisms ([Ben-tal and Nemirovski, 2002](#); [El Ghaoui et al., 1998](#)) or by generalizing the Soyster approach ([Bertsimas and Sim, 2004](#)). RO allows to solve decision-making problems under uncertainty even when the underlying probabilities are not known. It consists in immunizing a solution against adverse realizations of uncertain parameters within given uncertainty sets. The basic requirement for a robust solution is that constraints of the problem are not violated regardless of the realization of the parameters in the set. The issue then consists in identifying computable robust counterparts for the initial optimization program. [Ben-tal et al. \(2012\)](#) or [Bertsimas et al. \(2010\)](#) review techniques for building such robust counterparts in general cases.

Up until now, RO has not been used in IAMs, with the exceptions of [Babonneau et al. \(2011\)](#) and [Andrey et al. \(2015\)](#). A first contribution of our paper is to propose a general robust approach to consider uncertainty in simple climate models (SCMs) typically used by IAMs to represent climate evolution. Our approach relies on [Bertsimas and Sim \(2004\)](#). It consists in defining an uncertainty budget to control the degree of pessimism; in short, to limit the number of climate parameters allowed to deviate from their nominal values. We then rewrite the deterministic IAM to obtain its robust counterpart.

As an illustration, our approach is implemented in the TIAM-World integrated assessment model, which also relies on a SCM. We first define plausible uncertainty ranges for the climate parameters of the TIAM-World model and then calibrate these ranges using existing literature ([van Vuuren et al., 2009](#)) against climate simulations from the MAGICC model ([Meinshausen et al., 2011](#)). Then, using a robust counterpart of TIAM-World, a second contribution of this paper is to enrich the climate debate by defining robust energy transition pathways for different global warming targets. In other words, we identify economic transition pathways under climate constraints for which the outcome scenarios remain relevant for any realization of the climate parameters. Moreover, we can assess which climate parameter or which combination of climate parameters are the most sensitive in our model and we can quantify the uncertainty cost. The originality of our numerical results is that, unlike other studies (e.g., [Syri et al., 2008](#); [Labriet et al., 2015](#)), we consider uncertainty on all the climate system parameters of our IAM.

The remainder of this paper is organized as follows: we first present the approach in the general case (for all IAMs). We then describe how we implement our RO approach in the TIAM-World model and finally we present numerical results of selected scenarios and review the different insights brought by the RO approach and how it can inform policy makers.

## 2. General approach

### 2.1. Integrated assessment modelling

Integrated assessment models (IAMs) of climate change policies present different levels of integration ([Schneider, 1997](#)). Along this axis, there are again two ends to the spectrum. On one end, there are models such as the MIT IGSM ([Sokolov et al., 2005](#)) composed of loosely interconnected but more detailed (economic and climate, in particular) modules. At the other end, there are more integrated models such as TIAM-World. We believe that this second set of comprehensively integrated models are more amenable to uncertainty analyses.

A comprehensively integrated IAM can typically be cast as a single mathematical programming model, where a social planner would be assumed to maximize social welfare ( $f$ ), under constraints which could be economic, technical or social ( $g$ ) as well as climatic ( $h$ ):

$$\begin{cases} \max_x f(x) \text{ (social welfare)} \\ \text{s.t.} \\ g(x) \leq 0 \text{ (economic, technical or social constraints)} \\ h(x) \leq 0 \text{ (climatic constraints)} \\ x \in \mathbb{R}^n \end{cases} \quad (1)$$

The set  $h(x) \leq 0$  of climatic constraints minimally i) describes the Earth's carbon cycle to determine the atmospheric CO<sub>2</sub> concentration; ii) computes, using this concentration as well as other GHGs concentration (often exogenous), the Earth's radiative forcing balance; and iii) determines the evolution of the Earth's mean surface temperature. This constitutes the climate module typical of well-known IAMs such as DICE, FUND and MERGE. We shall refer to such a module as a simple climate model (SCM). By contrast, there are more complex climate models called Earth System Models of Intermediate Complexity (EMICs) such as C-GOLDSTEIN (Edwards and Marsh, 2005), which could take hours to run, or even full-fledged climate models called Atmosphere-Ocean Global Circulation Models (AOGCMs, see e.g. Boville et al., 2001), which could take weeks to run on a supercomputer.

In SCMs, the carbon cycle can be modelled in two main ways. It can be represented by different 'carbon boxes' (e.g., the atmosphere, the upper ocean and the lower ocean) with exchange rates as in DICE. Or it can be represented by an impulse-response function as in FUND and MERGE. Most SCMs do not have retroactions of the CO<sub>2</sub> concentration on the carbon cycle parameters. This is an obvious simplification as the CO<sub>2</sub> removal rate from the atmosphere is not constant due the finite uptake capacity of the ocean.

The modelling of radiative forcing ( $F$ ) is rather similar across SCMs. It is defined by the radiative forcing of each GHG considered ( $F_{\text{GHG}}$ ):

$$F(t) = \sum_{\text{GHG}} F_{\text{GHG}}(t) \quad (2)$$

Radiative forcing due to CO<sub>2</sub> is often defined by a logarithmic function of the actual atmospheric CO<sub>2</sub> concentration ( $M$ ):

$$F_{\text{CO}_2}(t) = \gamma \log_2 \left( \frac{M(t)}{M_0} \right) \quad (3)$$

This logarithmic function is sometimes linearized, as in TIAM-World. The main differences among SCMs are parameter values (e.g.,  $\gamma$  and  $M_0$ ) and the treatment of non-carbon dioxide GHGs (exogenously or not).

Change in radiative forcing translates in changes for the mean surface temperature ( $T_{at}$ ) and the mean (deep) ocean temperature ( $T_{oc}$ ) depending in particular on the assumed climate sensitivity. In SCMs, this is generally estimated using two linear equations:

$$T_{at}(t) = \mu(F(t), T_{at}(t-1), T_{oc}(t-1)) \quad (4)$$

$$T_{oc}(t) = \psi(T_{at}(t-1), T_{oc}(t-1)) \quad (5)$$

The main differences among SCMs are, again, parameter values and the functional form of  $\mu$  and  $\psi$ .

## 2.2. Uncertainty ranges

Differences among SCMs especially come from their choices of key parameters. It is thus important to define ‘appropriate’ uncertainty ranges for these parameters. This will help assess how robust SCMs are and understand which parameters or combinations of parameters are the most sensitive. Evaluating such ranges reveals several difficulties (see, e.g., Hof et al., 2012; Hu et al., 2012; Butler et al., 2014). First, as already mentioned, SCMs are designed to evaluate climate responses with limited computational burdens. They thus rely on some structural simplifications. For instance, most SCMs ignore carbon and climate feedbacks in their description of the carbon dynamics. Such simplifications induce bias. As an illustration, van Vuuren et al. (2009) show how differently carbon cycle can behave within a standard impulse-response experiment, depending on whether it includes or not feedbacks. Second, there is a parametric uncertainty due to the intrinsic volatility of the natural phenomena at stake, as well as the imperfection of measures and statistical estimations. As an illustration, Knutti and Hegerl (2008) exhibits different distributions and ranges for the climate sensitivity based on different lines of evidence. And third, there is a form of ‘selection bias’ due to heterogeneous degrees of information on parameters estimation and calibration. Overall, IAM-SCMs modellers may have a tendency to pay more attention to some parameters, based on available information.

## 2.3. Robust optimization approach

Let us consider again our basic IAM formulation:

$$(\mathbf{P}) : \begin{cases} \max_x f(x) \\ s.t. g(x) \leq 0 \\ h(x, a) \leq 0 \end{cases} \quad (6)$$

where  $x \in \mathbb{R}^n$  is a vector of decision variables, and  $a \in \mathbb{R}^m$  is a vector of uncertain parameters in  $h(x, a)$ . In what follows,  $h$  will be a temperature constraint. We assume that any realization  $a_i$  might take on of three values  $\{a_i^-, \bar{a}_i, a_i^+\}$ , each representing the lowest value, nominal value, and highest value, respectively. This uncertainty typically gives rise to the following space of possible candidates for  $a$ :

$$\mathbb{U} = \{a \in \mathbb{R}^m \mid \exists z^+ \in \{0, 1\}^m, z^- \in \{0, 1\}^m, z^+ + z^- \leq 1, a_i = \bar{a}_i + (a_i^+ - \bar{a}_i)z^+ + (a_i^- - \bar{a}_i)z^-\}$$

Following Bertsimas and Sim (2004), it is possible to control the degree of pessimism of the solution by allowing only a subset of parameters to deviate from their nominal values. The concept of the uncertainty budget is based on the fact that it is highly unlikely that all the parameters take one of their two extreme values at the same time. This motivates the use of the following robust counterpart of the initial problem:

$$(\mathbf{RC}) : \begin{cases} \max f(x) \\ s.t. g(x) \leq 0 \\ h(x, a) \leq 0, \forall a \in \mathbb{U}(\Gamma) \end{cases} \quad (7)$$

with

$$\mathbb{U}(\Gamma) = \left\{ a \in \mathbb{R}^m \mid \exists z^+ \in \{0, 1\}^m, z^- \in \{0, 1\}^m, z^+ + z^- \leq 1, \sum_i z_i^+ + z_i^- \leq \Gamma, a_i = \bar{a}_i + (a_i^+ - \bar{a}_i)z_i^+ + (a_i^- - \bar{a}_i)z_i^- \right\}$$

where  $\Gamma \in \{0, 1, 2, \dots, n\}$  is the maximum number of parameters taking one of their extreme values. The idea behind the robustification of  $h$  is that the solution of the energy-economy

problem should be feasible for any ‘nature-controlled’ realization of the uncertain parameters in e.g. the temperature constraint. Thus, we want to identify the worst-case combination of parameters in  $h$  constrained by the uncertainty budget  $\Gamma$ . For example, assuming we want to determine optimal economic mitigation choices to limit global warming below 2 °C, we need to identify trajectories that meet the temperature target even though some of the climate parameters were wrongly estimated. We assume that decisions shall be taken before the actual values of the parameters are known, to reflect the current status of political discussions and scientific progress in climate science.

Under linearity conditions of  $h(x, a)$  with respect to  $a$ , the uncertainty set  $\mathbb{U}(\Gamma)$  can be equivalently replaced with its convex hull<sup>2</sup>:

$$\mathbb{U}'(\Gamma) = \left\{ a \in \mathbb{R}^m \mid \exists z^+ \in [0, 1]^m, z^- \in [0, 1]^m, \begin{array}{l} z^+ + z^- \leq 1, \sum_i z_i^+ + z_i^- \leq \Gamma \\ a_i = \bar{a}_i + (a_i^+ - \bar{a}_i)z^+ + (a_i^- - \bar{a}_i)z^- \end{array} \right\}$$

and the robust constraint can be reformulated using strong duality as:

$$\begin{cases} h(x, \bar{a}) + \sum_i \max((a_i^- - \bar{a}_i)h'_i(x) - v; 0; (a_i^+ - \bar{a}_i)h'_i(x) - v) + \Gamma v \leq 0 \\ v \geq 0 \end{cases} \quad (8)$$

where  $v \in \mathbb{R}$  is an additional decision variable that need to be optimized jointly with  $x$ , and where  $h'_i(x)$  is the derivative of  $h(x, a)$  with respect to  $a_i$ .

The robust problem can then be reformulated by incorporating this new set of constraint in the original problem (see [Bertsimas and Sim, 2004](#), for the original discussion about such a reformulation). Unfortunately, such reformulations are not always possible. Beyond the strictly linear case, [Ben-tal et al. \(2012\)](#) proposes a methodology to reformulate robust programs in the more general case of nonlinear but still convex constraints when using convex uncertainty sets such as  $U'(\Gamma)$ . Yet, these conditions typically involve that both  $h(x, a)$  be concave in  $a$  and that the uncertainty set be a convex set. Unfortunately, the mere fact that  $h(x, a)$  be a concave function prevents one from replacing  $\mathbb{U}(\Gamma)$  with its convex hull. This implies that such reformulation are unlikely to be obtainable for robust non-linear climate constraints when an uncertainty set as  $\mathbb{U}$  is used.

As an illustration, let us consider that temperature follows some linear dynamics, i.e., Eq. (4) can be written as:

$$T_{at}(t) = a_1 F(t) + a_2 T_{at}(t-1) + a_3 T_{oc}(t-1),$$

where  $(a_1, a_2, a_3)$  are three parameters that might be considered uncertain. When unfolding this expression in order to assess the long term effect of the parameters on the temperature level, we get expressions of the form:

$$T_{at}(t) = \sum_{\tau=1}^t a_2^{t-\tau} a_1 F(\tau) + a_2^t T_{at}(0) + \sum_{\tau=1}^t a_2^{t-\tau} a_3 T_{oc}(\tau),$$

which is a polynomial function of  $(a_1, a_2, a_3)$  and does not in general satisfy structural assumptions such as monotonicity, convexity or concavity. This makes the hope of obtaining a compact reformulation as in (8) somewhat unrealistic.

Note that it is possible to avoid the need of a compact reformulation by including additional constraints that exhaustively enumerate all possible combination of deviations that need to be verified for a given choice of  $\Gamma$ . Unfortunately, the number of such combinations increases

---

<sup>2</sup>Refer to example 14.3.2.B in [Ben-tal et al. \(2009\)](#) for a proof of this representation.



exponentially with respect to  $m$ , the number of uncertain parameters. To avoid the exponential growth in the problem size, we suggest employing a constraint generation method that will attempt to identify a small subset of such extreme value combinations that are sufficient to obtain the optimal robust solution of the problem. This approach is fairly generic as it relies entirely on two modest (as we will see) assumptions: i) the ability to identify a worst-case combination of extreme value for a fixed decision  $x$ ; and ii) the ability to solve the RC problem where the robust constraint is replaced by:

$$h(x, a) \leq 0, \forall a \in \{\hat{a}_1, \hat{a}_2, \dots, \hat{a}_K\} \quad (9)$$

Let us now detail our proposed constraint generation algorithm:

1. Set  $\hat{\mathbb{U}}_1 = \{\bar{a}\}$  and  $k = 1$
2. Solve the master problem ( $MP(\hat{\mathbb{U}})$ ) which consists in maximizing the social surplus under a robust temperature constraint that accounts only for instances of the parameters  $a$  contained in  $\hat{\mathbb{U}}$ :

$$(MP(\hat{\mathbb{U}})) : \begin{cases} \max_x f(x) \\ s.t. \\ g(x) \leq 0 \\ h(x, a) \leq 0, \forall a \in \hat{\mathbb{U}} \\ x \in \mathbb{R}^n \end{cases}$$

Capture the optimal trajectories in this problem with  $x_k^*$ .

3. Given some optimal trajectories, identify the worst-case scenario in  $\mathbb{U}$  for the parameters of the temperature constraint function by solving the  $SP(x_k^*)$  worst-case analysis problem:

$$(SP(x_k^*)) : \left\{ \max_{a \in \mathbb{U}(\Gamma)} h(x_k^*, a) \right.$$

Capture the worst-case value of this problem as  $h_k^*$  and one of the assignments that achieve the worst-case value as  $a_k^*$ .

4. If  $h_k^* \leq 0$ , terminate the algorithm and return  $x_k^*$  as the optimal robust trajectories of problem (P) in Eq. (6). Otherwise, add  $a_k^*$  in the set  $\hat{\mathbb{U}}$ , increase  $k$  by one, and go to Step 2.

### 3. Application to TIAM-World

#### 3.1. TIAM-World

##### 3.1.1. Model overview

The TIMES Integrated Assessment Model (TIAM-World) is a detailed, global, multi-region technology-rich model of the energy/emission system of the world. It is based on the TIMES (The Integrated MARKAL-EFOM System) economic paradigm, which computes an inter-temporal dynamic partial equilibrium on energy and emission markets based on the maximization of total surplus<sup>3</sup>. TIAM-World is described in [Loulou \(2008\)](#) and in [Loulou and Labriet \(2008\)](#). It is

---

<sup>3</sup>A complete description of the TIMES equations appears in [www.etsap.org/documentation](http://www.etsap.org/documentation).

used in many international and European projects (for recent applications see: Babonneau et al., 2011; Labriet et al., 2012). The multi-region partial equilibrium model of the energy systems

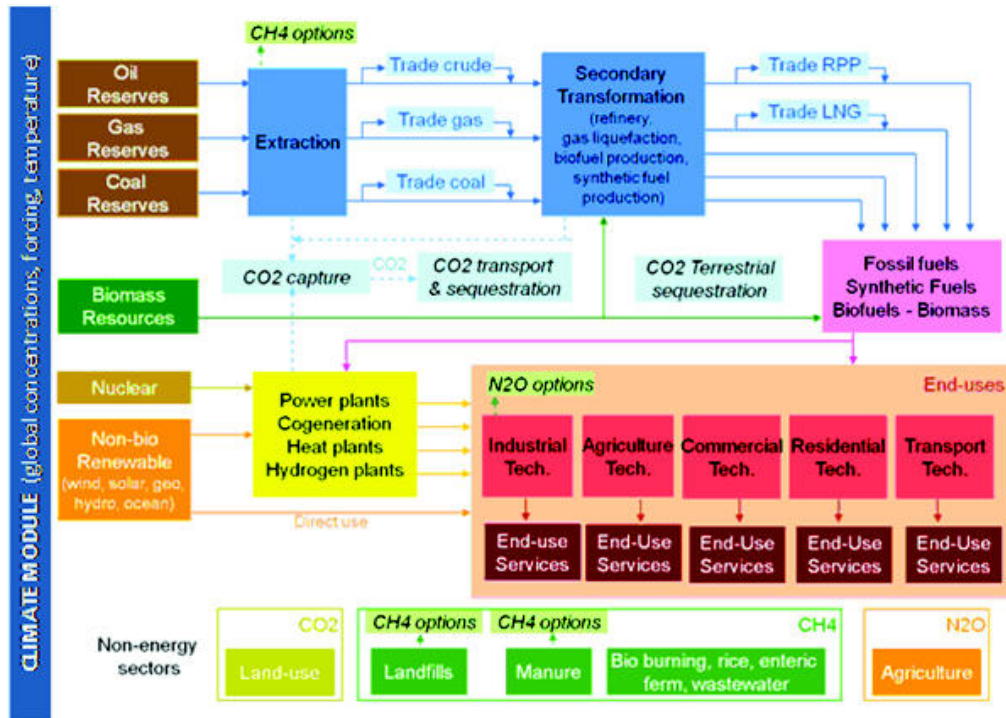


Figure 1: TIAM reference energy system

of the entire World is divided in 16 regions. Regions are linked by trade variables of the main energy forms (coal, oil, gas) and of emission permits. TIAM's planning horizon extends from 2000 to 2100, divided into periods of varying lengths.

In TIMES, an intertemporal dynamic partial equilibrium on energy markets is computed, where demands for energy services are exogenously specified (only in the reference case), and are sensitive to price changes in alternate scenarios via a set of own-price elasticities at each period. Although TIMES does not encompass all macroeconomic variables beyond the energy sector, accounting for price elasticity of demands captures a major element of feedback effects between the energy system and the economy. Thus, the equilibrium is driven by the maximization (via linear programming) of the discounted present value of total surplus, representing the sum of surplus of producers and consumers, which acts as a proxy for welfare in each region of the model (practically, the LP minimizes the negative of the surplus, which is then called the energy system cost).

The maximization is subject to many constraints, such as: supply bounds (in the form of supply curves) for the primary resources, technical constraints governing the use of each technology, balance constraints for all energy forms and emissions, timing of investment payments and other cash flows, and the satisfaction of a set of demands for energy services in all sectors of the economy.

The nominal formulation of the TIAM problem is a cost minimization and can be written as follows (with some simplifications):

$$\left\{ \begin{array}{l} \min \sum_t c_t^T x_t \\ s.t. \\ L_t x_t \geq b_t, x_t \in \mathbb{R}^n, L_t \in \mathbb{R}^{m^*n}, \text{ (technological constraints)} \\ D_t x_t \geq d_t, x_t \in \mathbb{R}^n, D_t \in \mathbb{R}^{d^*n}, \text{ (demand constraints)} \\ y_t \leq w_t, \text{ with } y_t = Ay_{t-1} + Fx_t, \text{ (recursive climate constraints)} \\ x_t \in \mathbb{R}^n, y_t \in \mathbb{R}^w, A \in \mathbb{R}^{w^*w}, F \in \mathbb{R}^{w^*n} \end{array} \right.$$

The objective function is the total cost of the system. It includes, among others: investment costs, operating costs of the various sectors, taxes, transportation costs between geographical zones... Technological constraints cover capacity limits, supply limits, yields, the allowed growth rates of the processes in the various sectors. Demand constraints include each zone's energy service demands and climate constraints embrace limits on GHG emissions or stocks in the atmosphere or on temperature increase. These latter constraints belong to an endogenous climate module. Note that the CO<sub>2</sub>, CH<sub>4</sub> and N<sub>2</sub>O emissions related to the energy sector are explicitly represented by the energy technologies included in the model. The nonenergy-related CO<sub>2</sub>, CH<sub>4</sub> and N<sub>2</sub>O emissions (landfills, manure, rice paddies, enteric fermentation, waste water, and land use) are also included in order to correctly represent the radiative forcing induced by them, but they are exogenously defined. Emissions from some Kyoto gases (CFCs, HFCs, and SF6) are not explicitly modelled, but a special radiative forcing term is added in the climate module.

### 3.1.2. The climate module

The climate module used in TIAM-World for this work is an adapted version of the model developed by [Nordhaus and Boyer \(1999\)](#). Greenhouse gas concentration and temperature changes are calculated from linear recursive equations. We briefly present its characteristics here, a detailed description can be found in [Loulou et al. \(2010\)](#).

The climate representation in TIAM-World is characterized by three steps. First, the GHGs emitted by anthropogenic activities accumulate in the atmosphere; exchanges with the upper and deep ocean layers occur then for CO<sub>2</sub>, while the dissipation of CH<sub>4</sub> and N<sub>2</sub>O is described with single atmospheric decay parameters. The terrestrial carbon cycle of this climate module is depicted in [Figure 2](#). Formally, the one-year-lagged dynamics of the three detailed greenhouse gases are the following (see [Appendix A](#) for detailed equations):

$$M_t^g = \Phi^g M_{t-1}^g + F E_t^g \quad (10)$$

where  $M_t^g$  is the vector of the mass of gas  $g$  across the different reservoirs in year  $t$ ,  $E_t^g$  is the emission of gas  $g$  in year  $t$  (from the global energy model),  $g \in G = \{\text{CO}_2, \text{CH}_4, \text{N}_2\text{O}\}$  and  $r : \text{reservoirs} \in R = \{\text{Atmosphere}, \text{UpperLayer}, \text{LowerLayer}\}$ . This set of equations defining the time profiles of atmospheric GHGs is then used to compute the radiative forcing. It is common to consider that forcings are additive, so that:

$$\Delta F_t = \sum_{g \in G} \Delta F_t^g + Exf_t \quad (11)$$

where  $\Delta F_t^g$  is the forcing of gas  $g$  in period  $t$  and  $Exf_t$  corresponds to an exogenous assumption of forcing for all gases other than carbon dioxide, methane and nitrous oxide. The current knowledge on radiative forcing suggests that none of these terms is linear in the atmospheric stock of gas; the linearization used here is proposed by [Loulou et al. \(2010\)](#):

$$\Delta F_t^g = \gamma_g A^g + \gamma_g B^g M_t^g, \quad (12)$$

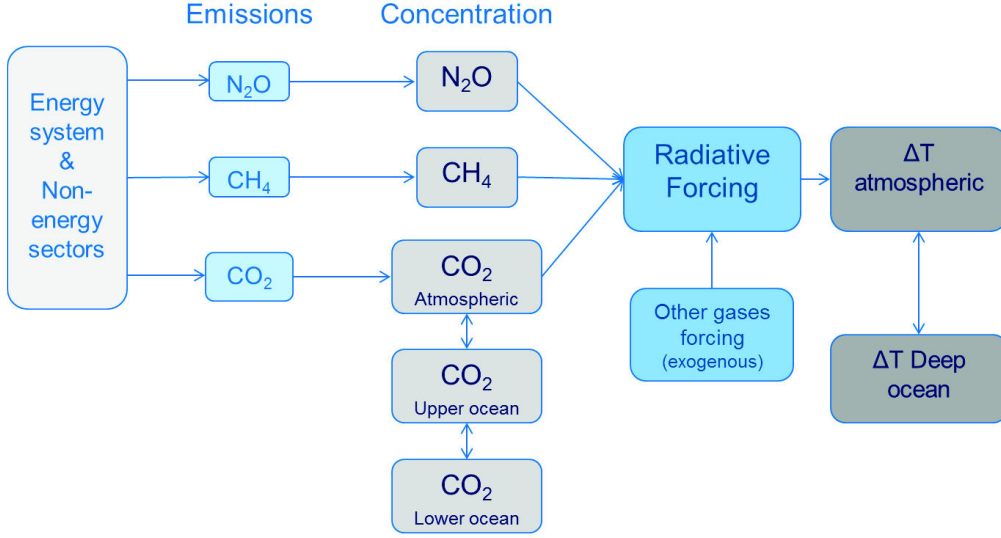


**Figure 2:** TIAM climate module

where  $\gamma$  is a constant (the radiative forcing sensitivity to atmospheric  $\text{CO}_2$  doubling for  $g = \text{CO}_2$ ), and A's and B's are constant depending on pre-industrial concentration levels and linearization intervals.

Finally, temperature elevation profiles are computed based on the following equations:

$$\begin{bmatrix} \Delta T^{up} \\ \Delta T^{lo} \end{bmatrix}_t = S \begin{bmatrix} \Delta T^{up} \\ \Delta T^{lo} \end{bmatrix}_{t-1} + \begin{bmatrix} \sigma_1 \\ 0 \end{bmatrix} \Delta F_t, \quad (13)$$

$$S = \begin{bmatrix} 1 - \sigma_1 \left( \frac{\gamma}{C_S} + \sigma_2 \right) & \sigma_1 \sigma_2 \\ \sigma_3 & 1 - \sigma_3 \end{bmatrix}.$$

where  $\Delta T^{up}$  is the variation of the atmospheric temperature,  $\Delta T^{lo}$  the variation of the ocean temperature,  $C_S$  represents the climate sensitivity, i.e. the change in equilibrium atmospheric temperature due to a doubling of GHG concentration;  $\sigma_1$  and  $\sigma_3$  are the adjustment speeds for respectively atmospheric and oceanic temperature (lags, in  $year^{-1}$ );  $\sigma_2$  is a heat loss coefficient from the atmosphere to the deep ocean.

### 3.2. Uncertainty sets

The concrete procedure for estimating min and max values for the climate system parameters differs across parameters. While most estimations are based on comparisons with existing literature (Stocker et al., 2013; Butler et al., 2014), the construction of lower and upper bounds for the three-box carbon cycle parameters relies on a calibration against existing emission scenarios and the subsequent concentrations from MAGICC6 (Meinshausen et al., 2011). More detail about the estimation procedures can be found in Appendix B; Table 1 lists the nominal values and upper/lower bounds for the TIAM climate model parameters. Instead of keeping an upper and a lower value for the parameters, a rapid pre-study provided us the worst-case value of the parameters (in bold letters in the table).

| Parameter    | Description                                                    | Nominal value | Lower bound    | Upper bound    |
|--------------|----------------------------------------------------------------|---------------|----------------|----------------|
| $\phi_{a-u}$ | Atmosphere to upper layer carbon transfer coefficient (annual) | 0.046         | <b>0.04393</b> | 0.04807        |
| $\phi_{u-a}$ | Upper layer to atmosphere carbon transfer coefficient (annual) | 0.0453        | 0.04326        | <b>0.0473</b>  |
| $\phi_{u-l}$ | Upper to lower layer carbon transfer coefficient (annual)      | 0.0146        | <b>0.0139</b>  | 0.01526        |
| $\phi_{l-u}$ | Lower to upper layer carbon transfer coefficient (annual)      | 0.00053       | 0.00051        | <b>0.00055</b> |
| $\gamma$     | Radiative forcing from doubling of $CO_2$                      | 3.7           | 2.9            | <b>4.5</b>     |
| $C_S$        | Climate sensitivity from doubling of $CO_2$                    | 2.9           | 1.3            | <b>4.5</b>     |
| $\sigma_1$   | Adjustment speed of atmospheric temperature                    | 0.024         | 0.0216         | <b>0.0264</b>  |
| $\sigma_2$   | Heat loss from atmosphere to deep ocean                        | 0.44          | <b>0.396</b>   | 0.484          |
| $\sigma_3$   | Heat gain by deep ocean                                        | 0.002         | <b>0.0018</b>  | 0.0022         |

**Table 1:** Nominal values and bounds for climate parameters

### 3.3. Robust formulation of the climate problem

Based on the uncertainty that was described above, one can describe a robust counterpart of TIAM as follows :

$$\left\{ \begin{array}{l} \min_x \sum_t c_t^T x_t \\ \text{s.t. } L_t x_t \geq b_t \quad (\text{technological constraints}) \\ \quad D_t x_t \geq d_t \quad (\text{demand constraints}) \\ \quad y_t(x, A, F) \leq w_t, \forall (A, F) \in \mathbb{U}(\Gamma) \quad (\text{robust temperature constraints}) \\ \quad x \in \mathbb{R}_+^n \end{array} \right.$$

where the climate equation is written as:

$$y_t(x, A, F) = \sum_{\tau=1}^t A^{t-\tau} F x_\tau + A^t y_0$$

and where intuitively the uncertainty set  $\mathbb{U}(\Gamma)$  includes any pair of matrices  $(A, F)$  that can be obtained by setting less than  $\Gamma$  of the uncertain parameters described in Table 1 to one of their extreme values. The algorithm described in Section 2.3 can be applied here as long as we are able to solve:

$$(SP(x_k^*)) : \left\{ \max_{(A, F) \in \mathbb{U}(\Gamma)} h(x_k^*, A, F) := \max_{t=1, \dots, T} y_t(x, A, F) - w_t, \right.$$

and return the maximum value with a pair  $(A_k^*, F_k^*)$  that achieves this worst-case value for one of the time period in the horizon  $t = 1, \dots, T$ .

This resolution will be done by enumerating through all  $t$ 's and identifying a worst-case  $(A_t^*, F_t^*)$  pair for:

$$\max_{(A,F) \in \mathbb{U}(\Gamma)} y_t(x, A, F) - w_t. \quad (14)$$

Given that the largest worst-case difference among all  $t$ 's is achieved at  $t^*$ , the oracle will return  $h_k^* := y_t(x, A, F) - w_t$  with the pair  $(A_{t^*}^*, F_{t^*}^*)$  to be included in  $MP(\hat{\mathbb{U}})$ . While it might be possible to solve problem (14) by enumerating through all the possible scenarios for  $A$  and  $B$ , we present in appendix C the procedure that we employed. It relies on the resolution of a mixed integer linear program which we believe might be more efficient when the number of uncertain parameters becomes large.

## 4. Numerical results

This section presents the results obtained with our robust version of TIAM-World. The uncertainty sets are given in Section 3.2 and the uncertainty budget takes value in  $[0 - 9]$  (9 being the number of uncertain parameters in the climate module). We consider two temperature limits for the whole 2000-2200 horizon: 2 °C and 3 °C. We will see that with the uncertainty-immunized solution, temperature paths are consistent with the limits considered by the Paris Agreement to the UNFCCC. We will first present temperature and GHG emission profiles, and then discuss energy transition pathways.

### 4.1. Temperature and emission trajectories

Figure 3 gives the temperature trajectories obtained with the nominal values of the climate parameters, when the trajectory with deviated parameters has to respect the 2 °C or 3 °C limit. They can be viewed as hedging trajectories: they should be followed in order to respect the temperature constraint even in presence of parameter uncertainty. Figure 3 reveals that uncertainty has a significant impact on the temperature trajectories, even for the uncertainty budget's low values. In order to ensure that the temperature does not exceed 2 °C (respectively, 3 °C), we should aim for a temperature increase ranged between 1.3 °C and 1.5 °C (resp., between 2 °C and 2.3 °C) with the nominal climate model in 2100. These new targets are consistent with the levels (1.5 °C and 2 °C) proposed by the Paris Agreement. Figure 3 reveals also that, to immunize against climate uncertainty with a 2 °C temperature limit, temperature peaks between 2060 and 2070 before decreasing rapidly. This notably impacts the energy transition pathways needed to respect these temperature levels; see Section 4.3. On the other hand, with a 3 °C temperature limit, temperature peaks only by the end of the century and decreases more slowly afterwards.

The robust optimization approach also makes it possible to rank the parameters or group of parameters by sensitivity. Table 2 shows the order in which climate parameters deviate, characterizing a diminishing negative impact on the temperature constraint. Since the robust counterpart of the nominal problem maximizes the temperature deviation for a given emission profile, increasing the uncertainty budget consists in finding parameters with the worst effect on the solution within the set of remaining (undeiated) parameters. The first deviating parameter is the climate sensitivity ( $C_S$ ). This can be explained by i) its wide uncertainty range compared to the ones of the other parameters and ii) the fact that it is a central parameter of the climate module. This is consistent with other studies analyzing climate response sensitivity to derive 2 °C-compliant mitigation pathways (Vanderzwaan and Gerlagh, 2006; Labriet

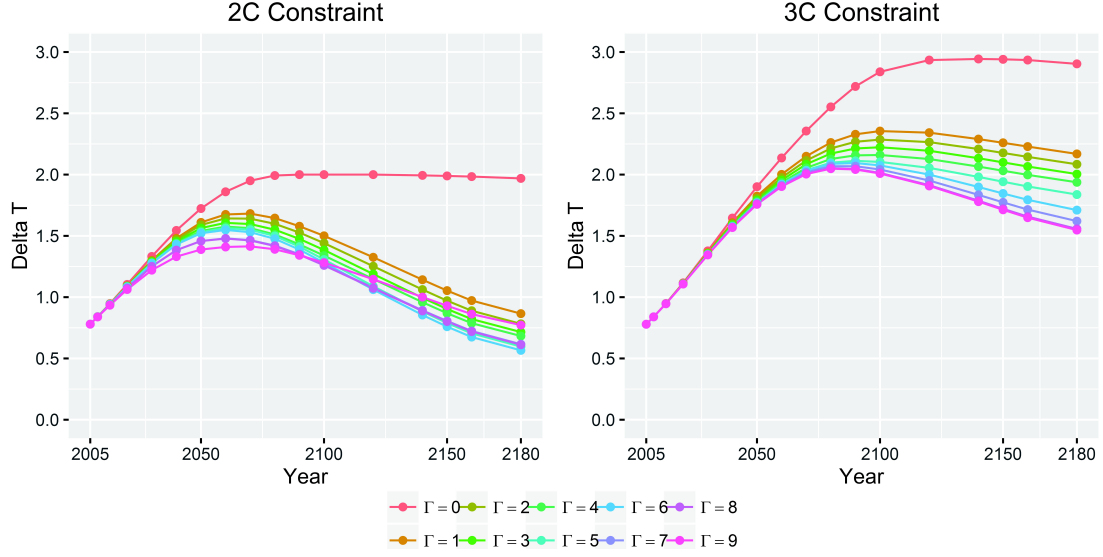


**Figure 3:** Atmospheric temperature trajectories for different values of the uncertainty budget

| Parameters | $C_S$ | $\phi_{a-u}$ | $\phi_{u-a}$ | $\sigma_2$ | $\gamma$ | $\sigma_1$ | $\phi_{u-l}$ | $\phi_{l-u}$ | $\sigma_3$ |
|------------|-------|--------------|--------------|------------|----------|------------|--------------|--------------|------------|
| Order 3 °C | 1     | 2            | 3            | 4          | 5        | 6          | 7            | 8            | 9          |
| Order 2 °C | 1     | 2            | 3            | 4          | 9        | 7          | 5            | 6            | 8          |

**Table 2:** Deviation order of uncertain climate parameters

et al., 2010; Ekholm, 2014). More interestingly, after the climate sensitivity the most critical parameters are the ones of the carbon cycle ( $\phi_{a-u}$  and  $\phi_{u-a}$ ). The terrestrial carbon dynamics is indeed of primary importance to assess the impact of anthropogenic GHG emissions, as it influences directly the atmospheric carbon concentration, and hence the radiative forcing and the temperature. This strengthens the importance of relying on appropriate uncertainty ranges for the climate parameters; see Appendix B. This also pleads for the necessity to pay more attention in IAMs to the intricacies of the carbon cycle, including feedbacks and nonlinearities. While climate sensitivity and the carbon cycle appear as primary factors, second-order parameters are ranked very differently. This may be (at least partially) explained by the mitigation dynamics in the two climate scenarios: in the 2 °C case, mitigation pathways must be implemented earlier (see the next figure) such that the climate dynamics does not have the same overall impact.

Figure 4 displays next CO<sub>2</sub> emission trajectories for the nominal scenarios and emission ranges in the robust scenarios.

In the nominal trajectories, emissions peak by the middle of the century in the 3 °C case, and decreases rapidly afterwards. Whereas in the 2 °C case, emissions must decrease rapidly from 2020 on<sup>4</sup>. Looking at the range of robust trajectories (shaded areas), it roughly expands over time in the 3 °C case to reach a maximum size by 2080; whereas in the 2 °C case, it reaches its maximum size earlier (2040). These dynamics are necessary to respect the different temperature

<sup>4</sup>Positive emissions in 2100 corresponds to a steady-state level, consistent with the temperature target, given the past emission trajectories.

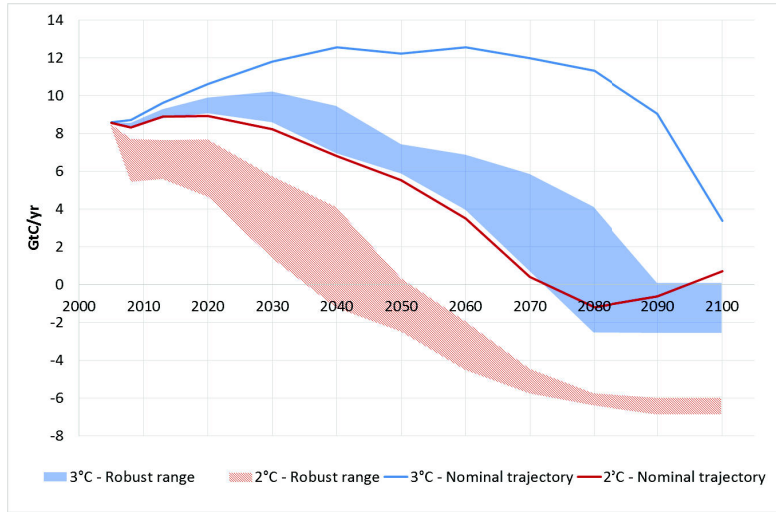


**Figure 4:** CO<sub>2</sub> emission profiles in the nominal and robust scenarios

profiles and implies contrasted energy transition pathways (both in terms of transition timing and energy portfolios); see Section 4.3. Note also the presence of negative emissions due to specific energy systems (see again Section 4.3).

## 4.2. Robustness cost

Let us now assess how the introduction of uncertainty impacts the total energy system cost (TIAM-World’s objective function), which yields the robustness cost. More precisely, we assess the trade-off between optimality (low system cost) and robustness (high uncertainty budget) by plotting in Figure 5 the cost increase with the ‘insurance’ level. It has been constructed through Monte-Carlo simulations, using the emission trajectories obtained for each value of  $\Gamma$  with a temperature constraint ( $T_{lim}=2^\circ\text{C}$  or  $3^\circ\text{C}$ ). The climate model parameters considered are uniformly distributed on the previously defined uncertainty sets. We are then able to derive the VaR and the CVaR for the temperature deviation in 2100 for both constraints. On the abscissa, we report the temperature deviation against which we ‘insure’ ourselves using the optimal robust pathway:  $x(T_{lim}, 2100, \Gamma) = CVaR(T_{lim}, 2100, 0) - CVaR(T_{lim}, 2100, \Gamma)$ ; see Appendix D for plots of the distributions obtained. The ordinate represents the objective function obtained for different value of the protection level normalized by the deterministic case objective function.

Figure 5 depicts how the world energy system and its emissions adapt to increasing protection levels with respect to a reference temperature target. It reads as the cost increase to support in order to ‘buy’ a certain amount of protection level given the uncertain response of the climate system: insuring against the risk that the 5%-CVaR of the average temperature increase will not be higher than  $xx$  (or reducing it by  $xx$  compared to the nominal case).

This function aggregates two elements, namely: (i) the evolution of the total energy system cost with an increasing uncertainty budget; and (ii) the CVaR-computed protection level associated to the change in global GHG emissions trajectory. Both are by construction concave functions of the uncertainty budget  $\Gamma$ . Indeed, the robust hedging strategies are driven by a worst-case logic, which implies that the incremental cost of increasing the uncertainty budget is necessarily diminishing. The same principle applies to GHG emissions. Interestingly, the process of composing these two functions yields a convex-shaped function. This implies that although



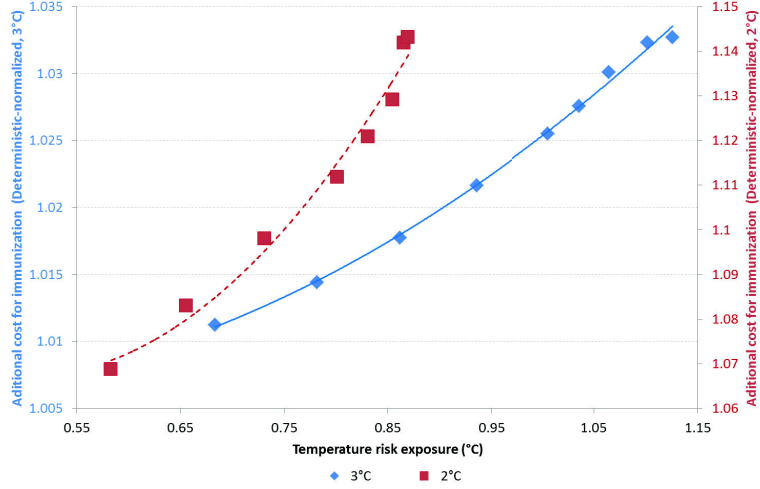


**Figure 5:** Costs of insurance

both the temperature-expressed protection level and the incremental cost are concave shaped, the incremental cost still grows faster than the temperature hedge acquired.

Overall, this plot is comparable to a ‘standard’ temperature-based marginal abatement cost curve, except that it embeds a consistent risk perspective which combines robust optimization and a simple CVaR metrics for the output GHG emissions pathways. Comparing the two series for different climate constraints, it appears naturally that costs of protection are higher for the 2 °C series, and also more convex, yielding higher marginal costs.

### 4.3. Robust energy transition pathways

Increasing the required protection level for a given nominal temperature target implies an adaptation of the energy system towards lower GHG emission levels. This section describes salient elements of these robust energy transition pathways.

#### 4.3.1. Robust decarbonization challenges: A mesoscopic view

Figure 6 plots the world primary energy<sup>5</sup> intensity of GDP, in 2050 and 2100, for the 3 °C and 2 °C targets (2050: plain lines, 2100: dashed lines; 3 °C: blue dot markers, 2 °C: red square markers) as a function of the protection level and 2008 normalized<sup>6</sup>. With the same convention, Figure 7 plots the evolution of the carbon intensity of primary energy with the protection level<sup>7</sup>.

The evolution of these two intensities reflects very different strategies for the 3 °C and 2 °C constraints. Hedging against climate uncertainty at the 3 °C level shows a balanced use of energy efficiency and decarbonization of primary energy in 2050; the two indicators show comparable

<sup>5</sup>Primary energy consumptions are computed as the sum of coal, crude oil, natural gas, enriched uranium, biomass, solar and wind energy consumed in the whole energy system.

<sup>6</sup> $PEI_{ratio} = \frac{Primary\_Energy(Yr)}{GDP(Yr)} \times \frac{GDP(2008)}{Primary\_Energy(2008)}$

<sup>7</sup> $CI_{ratio} = \frac{CO_2(Yr)}{Primary\_Energy(Yr)} \times \frac{Primary\_Energy(2008)}{CO_2(2008)}$

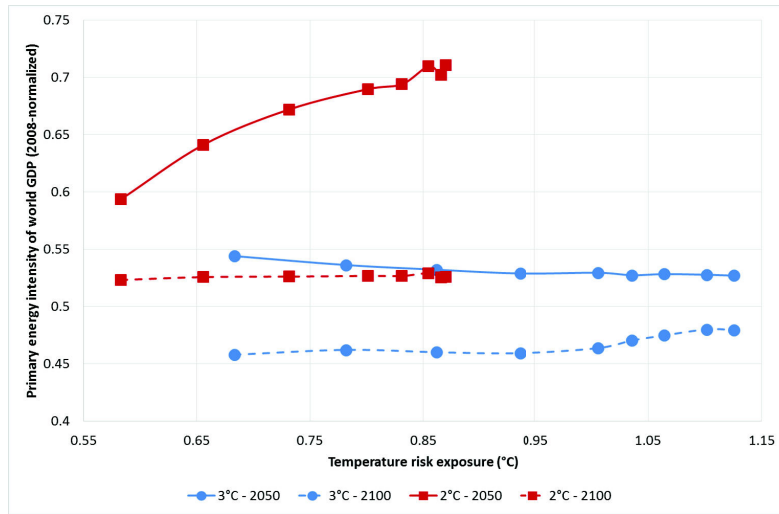


**Figure 6:** Primary energy intensity of GDP against protection level

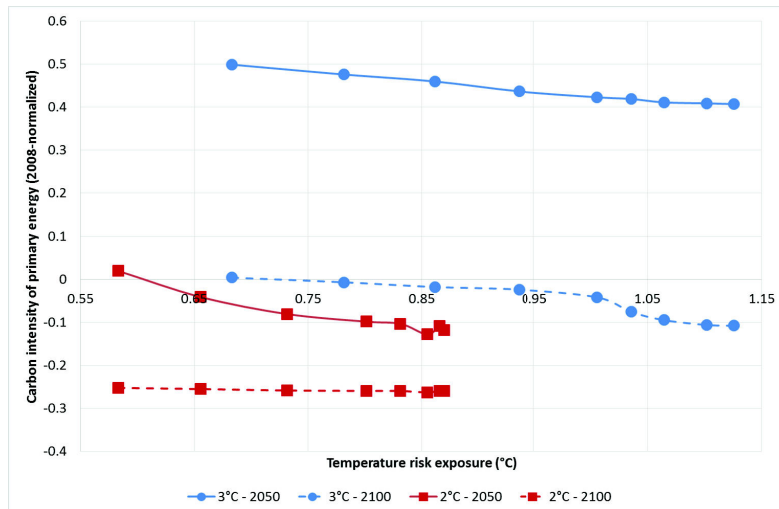


**Figure 7:** Carbon intensity of primary energy against protection level

reduction levels (more or less 50%) compared to the 2008 reference. In 2100, the 3 °C scenario hedges with a stronger reduction of carbon intensity, at the expense of primary energy intensity: carbon intensity drops with hedging (-50% to -60%) while energy intensity remains quite flat (-45% to -47%). This is especially true for higher protection levels for which CCS massively penetrates the decarbonization mix (see below). This yields negative carbon intensities, indicating negative net emissions. CCS-ready technologies being less efficient than their non-CCS equivalents, the primary energy requirements increase (moderately) with hedging.

At the 2 °C level, the tradeoff between energy intensity and carbon intensity is anticipated as early as 2050. With increased protection levels, the fall of primary energy intensity of GDP is less (from -40% to -30% compared to 2008), while the carbon intensity of GDP is reduced by an additional 10% going to negative values and hence negative net emissions. By 2100, protection

strategies have reached a status-quo situation with the amount of climatic uncertainty. Both the primary energy intensity and the carbon intensity have become insensitive to the protection level. The maximum abatement potential is thus reached (reflecting the model limits).

Overall, between the two climate scenarios, comparable strategies are chosen (tradeoff between energy intensity and carbon intensity, with the necessity to spend more energy to store carbon) but with a large difference in timing. This result is consistent with the temperature observation and CO<sub>2</sub> emissions paths, which show that protection at the 3 °C level is an *endpoint* issue (mitigation occurs in the second half of the century), while protection at the 2°C level is a *midpoint* question (mitigation is extremely strong by 2050, but final states – 2100 – show less variability). This raises the question of the economy’s decarbonization speed, and how to reach e.g. COP21 compliant objectives.

#### 4.3.2. Robust energy portfolios

While the previous results show an aggregate picture of reduction and mitigation strategies in an uncertain climate context, further desegregating the primary energy consumption level (see Figure 8) offers additional insights.

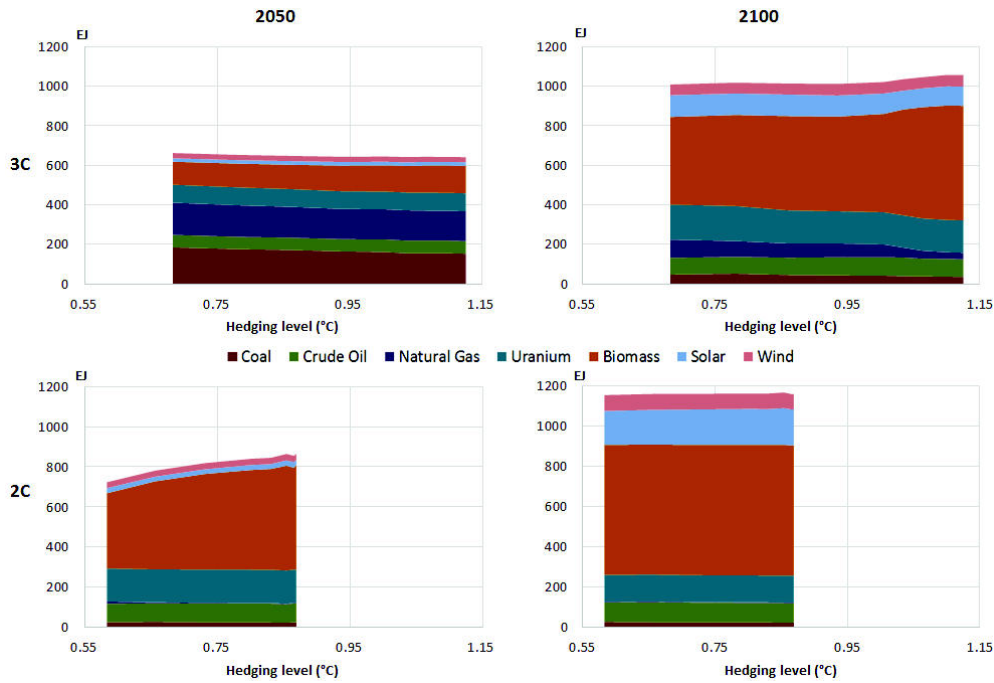


**Figure 8:** Primary energy consumption by type against protection level

Both the 3 °C and the 2 °C scenario groups show similarities. Naturally, increasing protection and/or imposing a more stringent climate objective tend to reduce the use of the most carbonized energy sources (coal, gas) in favour of renewable energy sources (solar, wind, biomass) (see also Figure 9).

As primary energy sources with high carbon contents, gas and coal uses are highly elastic to the protection level. Gas use decreases between 13% and 20% in 2050 and between 32% and 75% in 2100 in the 3 °C scenarios (always compared to the deterministic case in the same target

| EJ/yr |                                   | 3°C target  |           |      |         |         |       |      |               |           |       |
|-------|-----------------------------------|-------------|-----------|------|---------|---------|-------|------|---------------|-----------|-------|
|       |                                   | Natural Gas | Crude Oil | Coal | Uranium | Biomass | Solar | Wind | Non Renewable | Renewable | Total |
| 2050  | Deterministic                     | 189         | 62        | 237  | 54      | 97      | 16    | 26   | 542           | 139       | 681   |
|       | Lowest Protection level (0.68°C)  | 163         | 63        | 185  | 91      | 116     | 17    | 27   | 502           | 160       | 663   |
|       | Highest Protection level (1.13°C) | 151         | 63        | 153  | 91      | 139     | 18    | 26   | 458           | 184       | 642   |
| 2100  | Deterministic                     | 135         | 55        | 100  | 191     | 304     | 97    | 52   | 482           | 453       | 935   |
|       | Lowest Protection level (0.68°C)  | 93          | 84        | 47   | 177     | 444     | 110   | 55   | 401           | 608       | 1009  |
|       | Highest Protection level (1.13°C) | 34          | 89        | 36   | 164     | 580     | 98    | 58   | 322           | 735       | 1057  |
| EJ/yr |                                   | 2°C target  |           |      |         |         |       |      |               |           |       |
|       |                                   | Natural Gas | Crude Oil | Coal | Uranium | Biomass | Solar | Wind | Non Renewable | Renewable | Total |
| 2050  | Deterministic                     | 49          | 140       | 90   | 176     | 154     | 20    | 26   | 455           | 200       | 655   |
|       | Lowest Protection level (0.58°C)  | 12          | 91        | 24   | 164     | 376     | 25    | 30   | 292           | 431       | 723   |
|       | Highest Protection level (0.88°C) | 3           | 95        | 22   | 165     | 521     | 27    | 32   | 286           | 580       | 866   |
| 2100  | Deterministic                     | 34          | 131       | 58   | 133     | 409     | 105   | 60   | 356           | 574       | 930   |
|       | Lowest Protection level (0.58°C)  | 3           | 97        | 25   | 134     | 647     | 168   | 79   | 259           | 894       | 1153  |
|       | Highest Protection level (0.88°C) | 3           | 96        | 21   | 134     | 649     | 179   | 77   | 254           | 905       | 1159  |

**Figure 9:** Primary energy consumption by type

scenario group). At the same time, coal use is diminished by 22% to 36% in 2050 and 53% to 65% in 2100. The scenarios for the 2 °C target show a comparable albeit amplified tendency: both energy source uses diminish by 75% to 90% in 2050 and 2100. At the same time, the use of renewable energy raises in any case, up to 200% in 2050 for the 2 °C scenarios. While for the 3 °C scenarios, renewable use is tripled between 2050 and 2100. In the renewable group, biomass plays a particular role as its use coupled with CCS is a critical pathway for decarbonization (as it generates negative emissions).

Nuclear is an option for decarbonizing the economy, and more precisely an electro-intensive economy which relies more on carbon-neutral sources. The use of uranium gradually increases by 2100 in the 3 °C scenarios, and much faster in the 2 °C scenarios (up to 2050) before stabilizing. Lastly, oil plays a particular role: while the use of other fossil energy decreases, the amount of crude oil consumed in the primary energy mix is rather stable across scenarios and protection levels. This tendency to maintain the use of oil products is to be related to the difficulty of reducing transport emissions (high abatement costs) combined with the large availability of low-carbon alternatives in other sectors (nuclear, CCS).

#### 4.3.3. A sectoral view: The 'backstop' negative emissions pathways against low-elastic transport

Figure 10 helps next to assess the role of the various sectors in the decarbonization process.

Regardless of the scenario, transport remains the main CO<sub>2</sub> emitter worldwide. In the 3 °C case, all emissions peak around 2040 before falling – with the exception of the transport sector – alternative technologies penetrate the mix. Electricity and industry are the main contributors to abatement, essentially between 2050 and 2100. In 2100, transport emissions represent between 60% and 90% of the end-use emissions; they are rather stable in absolute terms, so that technology

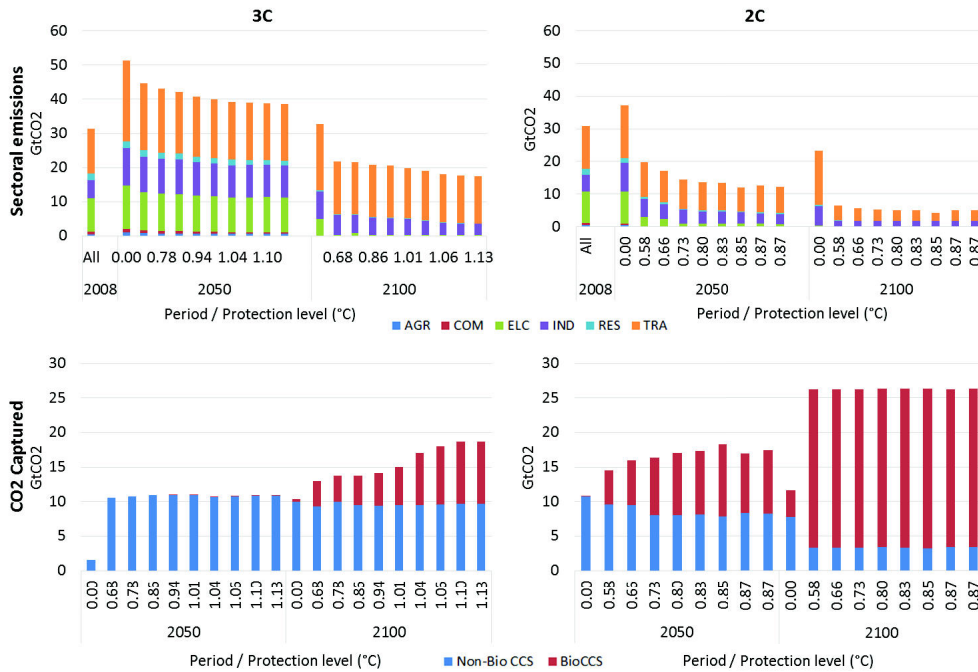


**Figure 10:** Sectoral emissions and Stored Carbon (from biomass and fossil fuels)

improvements (efficiency, low-carbon fuels) compensate for the demand growth. While CCS is deployed by 2050 as a hedge for about 10 Gt/yr, transport emissions in the second half of the century are compensated by credits from CCS captured from biomass (negative emissions).

The 2 °C case differs in three ways. First, the need to reduce emissions further to remain compliant with a 2 °C target with uncertainty forces to reduce emissions from the power and industry sectors much faster (by 2050). Second, even transport emissions go down sharply to get to a 1.5 °C average elevation level. At this timescale, only transport and industry have some residual emissions. Third, the additional use of CCS from biomass fueled power plants is not only incremental but also comes as a substitute for fossil CCS pathways. The importance of bioCCS in this picture reveals the importance of estimating biomass potentials and assessing relevant sensitivity analysis on the subject.

The clear-cut arbitrage strategy between biomass-CCS and transport emissions can be explained at the technology level, see Figure 11.

The analysis of the energy mix for transport shows a strong reliance on fossil-based fuels, which represent a large part of the mix except in the longer term for the 2 °C target. In that case, transport fuels have become almost carbon free with a strong reliance on hydrogen. Since transport is a sector with high abatement costs (Waisman et al. (2013)), it is only when uncertainty is high that the oil trajectory is impacted. The vehicle fleet is progressively electrified, diesel and gasoline losing market share with time and uncertainty. Electric vehicles appear as a relevant way to mitigate the risk induced by climate uncertainty. Besides, in energy terms, the moderate penetration of electricity as a transportation fuel minimizes a wider reality: while electricity can represent up to 30% of the energy used in transport, the relative efficiency of electric vehicles compared to conventional ones (2 to 2.5 more efficient) implies that, in 2050, more than 50% of the total world mobility is actually electromobility. Yet, the commercial

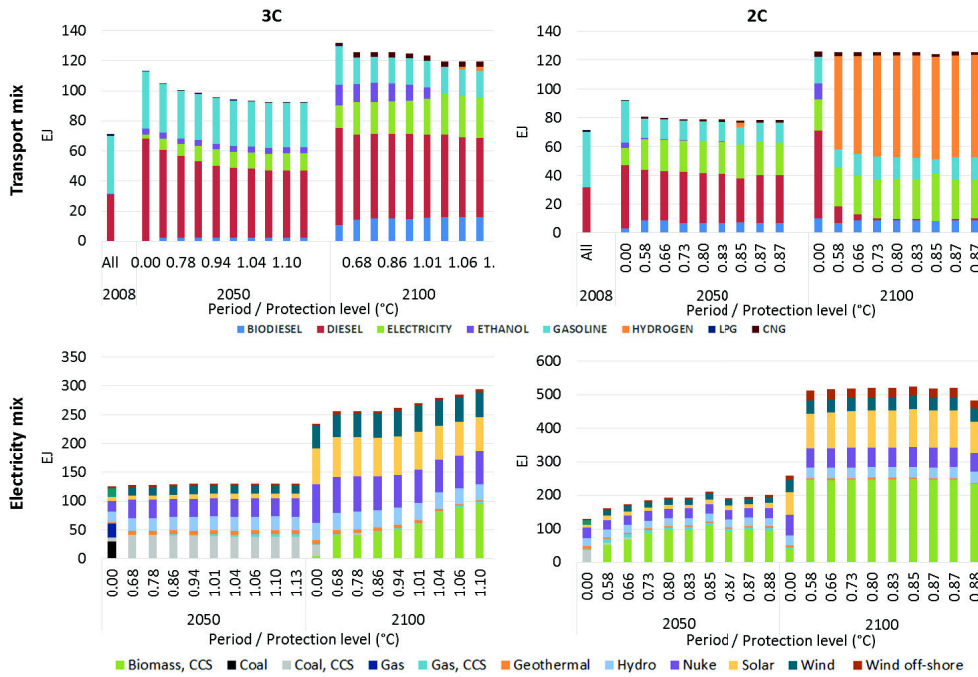


Figure 11: Energy mix for transport and electricity generation

transportation fleet sticks with diesel trucks, leading to a stable diesel consumption.

In the power sector, the introduction of uncertainty leads to an early use of CCS, as early as 2030 in most cases (see also Figure 10). The nuclear and the CCS trajectories under uncertainty have large consequences in terms of policy decision. For example, given the current state of R&D on CCS (with various projects shut down this last decade), this result suggests that we may want to reconsider the current R&D budget allocation. The importance of nuclear in the energy mix is also at odds with some country policies like Germany. Indeed, they decided some years ago to close all the nuclear plants in a near future (unlike Japan, where nuclear plants are planned to restart in the near future). Negative emission possibility is also something quite abstract and subject to much uncertainty, as the first commercial-scale biomass-fueled power plant with CCS has yet to be built.

## 5. Conclusion

Climate modeling is hampered by a considerable amount of uncertainty because of the lack of knowledge of the climate system. As it significantly impacts climate policy making, the need for tools to evaluate robust transition pathways is more and more urgent. In this paper, we present a robust approach to handling climate uncertainty in Integrated Assessment Models (IAMs).

We find that the climate module's most sensitive parameter is the climate sensitivity. This is consistent with the existing literature on the subject. Yet, it is important to remember that climate sensitivity is the most studied parameters and that its value estimations are numerous. Hence, the determination of the climate sensitivity uncertainty range is quite straightforward. Another important point is that this range relies on a large information set unlike the other parameters, for which data is scarce. It is indeed quite complicated to find information on

the carbon cycle parameters (few studies in the IAMs climate module literature) and yet the global climate system behavior is very sensitive to them. Furthermore, the parameters impact diversely the timing of the adaptation: the radiative forcing sensitivity multiplies directly the CO<sub>2</sub> concentration, hence even a small variation of this parameter leads to a strong impact on the CO<sub>2</sub> abatement timing. We then believe that a stronger focus should be put on the other climate model parameters.

To ensure that we comply with a 3 °C constraint, the temperature trajectories we should aim at with the nominal parameters should not exceed 2.4 °C, leading to zero net carbon emissions at the end of the century. With a 2 °C constraint, we should aim at 1.6 °C with negative carbon emissions as soon as 2050. If the insurance cost is quite reasonable for the higher constraint (from 1.5% to 4% of the system total discounted cost), it is less the case with a 2 °C objective. In the latter situation, the system total discounted cost increases by 7% when uncertainty is low and up to 14% when it is high. Indeed, in order to comply with a stringent target, sectors with high abatement costs have to participate in the global reduction effort. Transport is little impacted by the 3 °C target (but as uncertainty grows, the vehicle fleet is slightly modified), whereas the introduction of uncertainty leads to major fuel consumption changes for the 2 °C constraint.

The abatement strategies are quite different between the two temperature targets. For the 3 °C target, both the carbon intensity and the primary energy intensity of the economy decrease with uncertainty whereas for the 2 °C target, the energy intensity increases and the carbon intensity decreases. This more stringent goal is reached by investing massively in carbon removal technologies such as bioenergy with carbon capture and storage (BECCS) which have yields much lower than traditional fossil fueled technologies. Another interesting fact of the 2 °C hedging trajectories is the drastic increase in the nuclear electricity production. The massive use of nuclear or carbon removal technology is highly uncertain as BECCS is a very expensive technology that is not competitive in the absence of a high CO<sub>2</sub> price, while the development of the nuclear industry could be hampered by social acceptance issues. The 1.5 °C objective mentioned during the COP21 is obviously very ambitious and reaching it would necessitate strong political and societal ambitions and actions (much stronger than the ones decided during COP21).

By taking a robust approach to study ways of complying with ambitious climate targets, we were able to bring to light hedging technological trajectories without excessive computational issues. The method presented being quite generic, it could be interesting to perform similar exercises with other IAMs. It would help strengthen the knowledge on technological transition pathways with uncertainty and would allow a better understanding and awareness of the costs of the risks linked to our partial knowledge of the climate system.

## Bibliography

- Andrey, C., Babonneau, F., Haurie, A., Labriet, M., 2015. Modélisation stochastique et robuste de l'atténuation et de l'adaptation dans un système énergétique régional. Application à la région Midi-Pyrénées. *Natures Sciences Sociétés* 23 (2), 133–149.
- Anthoff, D., Tol, R. S. J., 2013. The uncertainty about the social cost of carbon: A decomposition analysis using FUND. *Climatic Change* 117 (3), 515–530.
- Babonneau, F., Kanudia, A., Labriet, M., Loulou, R., Vial, J.-P., Jul. 2011. Energy Security: A Robust Optimization Approach to Design a Robust European Energy Supply via TIAM-WORLD. *Environmental Modeling & Assessment* 17 (1-2), 19–37.
- Bahn, O., Chesney, M., Gheysens, J., Knutti, R., Pana, A. C., Apr. 2015. Is there room for geoengineering in the optimal climate policy mix? *Environmental Science & Policy* 48, 67–76.
- Ben-tal, A., El Ghaoui, L., Nemirovski, A., 2009. *Robust Optimization*. Princeton Series in Applied Mathematics. Princeton University Press.
- Ben-tal, A., Hertog, D. D., Vial, J.-P., 2012. Deriving robust counterparts of nonlinear uncertain inequalities.
- Ben-tal, A., Nemirovski, A., 2000. Robust solutions of Linear Programming problems contaminated with uncertain data. *Mathematical Programming* 88 (3), 411–424.
- Ben-tal, A., Nemirovski, A., 2002. *Robust Optimization — Methodology and Applications*. *Mathematical Programming* 92 (3), 453–480.
- Bertsimas, D., Brown, D. B., Caramanis, C., 2010. Theory and applications of Robust Optimization. *SIAM Review* 53 (3), 464–501.
- Bertsimas, D., Sim, M., Feb. 2004. The Price of Robustness. *Operations Research* 52 (1), 35–53.
- Block, K., Mauritsen, T., 2013. Forcing and feedback in the mpi-esm-lr coupled model under abruptly quadrupled co2. *Journal of Advances in Modeling Earth Systems* 5 (4), 676–691.
- Boville, B. A., Kiehl, J. T., Rasch, P. J., Bryan, F. O., Jan. 2001. Improvements to the NCAR CSM-1 for Transient Climate Simulations. *Journal of Climate* 14, 164–179.
- Butler, M. P., Reed, P. M., Fisher-Vanden, K., Keller, K., Wagener, T., 2014. Identifying parametric controls and dependencies in integrated assessment models using global sensitivity analysis. *Environmental Modelling & Software* 59, 10–29.
- Cao, L., Bala, G., Caldeira, K., Nemani, R., Ban-Weiss, G., 2010. Importance of carbon dioxide physiological forcing to future climate change. *Proceedings of the National Academy of Sciences of the United States of America* 107 (21), 9513–9518.
- Edwards, N. R. b. a., Marsh, R. b. a., 2005. Uncertainties due to transport-parameter sensitivity in an efficient 3-d ocean-climate model (english). *Climate dynamics* 24 (4), 415 – 433.
- Ekholm, T., 2014. Hedging the climate sensitivity risks of a temperature target. *Climatic Change* 127 (2), 153–167.
- El Ghaoui, L., Oustry, F., Lebret, H., 1998. Robust solutions to uncertain semidefinite programs. *Society for Industrial and Applied Mathematics* 9 (1), 33–52.
- Hof, A. F., Hope, C. W., Lowe, J., Mastrandrea, M. D., Meinshausen, M., van Vuuren, D. P., 2012. The benefits of climate change mitigation in integrated assessment models: The role of the carbon cycle and climate component. *Climatic Change* 113 (3-4), 897–917.



- Hope, C. W., 2006. The marginal impact of CO<sub>2</sub> from PAGE2002: An integrated assessment model incorporating the IPCC's five reasons for concern. *Integrated Assessment Journal* 6 (1), 19–56.
- Hu, Z., Cao, J., Hong, L. J., 2012. Robust Simulation of Global Warming Policies Using the DICE Model. *Management Science* 58 (December 2012).
- IPCC, 2007. In: Solomon, S., Qin, D., Manning, M., Chen, Z., Marquis, M., Averyt, K., Tignor, M., Miller, H. (Eds.), *Contribution of Working Group I to the Fourth Assessment Report of the Intergovernmental Panel on Climate Change*. Cambridge University Press, Cambridge, United Kingdom and New York, NY, USA.
- IPCC, 2014. Summary for policymakers. In: Field, C., Barros, V., Dokken, D., Mach, K., Mastrandrea, M., Bilir, T., Chatterjee, M., Ebi, K., Estrada, Y., Genova, R., Girma, B., Kissel, E., Levy, A., MacCracken, S., Mastrandrea, P., White, L. (Eds.), *Climate Change 2014: Impacts, Adaptation, and Vulnerability. Part A: Global and Sectoral Aspects. Contribution of Working Group II to the Fifth Assessment Report of the Intergovernmental Panel on Climate Change*. Cambridge University Press, Cambridge, United Kingdom and New York, NY, USA, pp. 1–32.
- Joos, F., Roth, R., Fuglestedt, J. S., Peters, G. P., Enting, I. G., Von Bloh, W., Brovkin, V., Burke, E. J., Eby, M., Edwards, N. R., Friedrich, T., Frölicher, T. L., Halloran, P. R., Holden, P. B., Jones, C., Kleinen, T., Mackenzie, F. T., Matsumoto, K., Meinshausen, M., Plattner, G. K., Reisinger, a., Segsneider, J., Shaffer, G., Steinacher, M., Strassmann, K., Tanaka, K., Timmermann, a., Weaver, a. J., 2013. Carbon dioxide and climate impulse response functions for the computation of greenhouse gas metrics: A multi-model analysis. *Atmospheric Chemistry and Physics* 13 (5), 2793–2825.
- Knutti, R., Hegerl, G. C., 2008. The equilibrium sensitivity of the Earth's temperature to radiation changes. *Nature Geoscience* 1 (11), 735–743.
- Labriet, M., Kanudia, A., Loulou, R., Dec. 2012. Climate mitigation under an uncertain technology future: A TIAM-World analysis. *Energy Economics* 34, S366–S377.
- Labriet, M., Loulou, R., Kanudia, A., Nov. 2010. Uncertainty and Environmental Decision Making. Vol. 138 of *International Series in Operations Research & Management Science*. Springer US, Boston, MA.
- Labriet, M., Nicolas, C., Chung-Ming, S., Kanudia, A., Loulou, R., 2015. Energy decisions in an uncertain climate and technology outlook : how stochastic and robust analyses can assist policy-makers. In: Giannakidis, G., Labriet, M., Gallachóir, B. O., Tosato, G. (Eds.), *Informing energy and climate policies using energy systems models*, Springer s Edition. Springer, Ch. 03.
- Loulou, R., 2008. ETSAP-TIAM: the TIMES integrated assessment model. part II: mathematical formulation. *Computational Management Science*, 5 (1), 41–66.
- Loulou, R., Labriet, M., 2008. ETSAP-TIAM: the TIMES integrated assessment model Part I: Model structure. *Computational Management Science*, Special issue "Managing Energy and the Environment 5 (1).
- Loulou, R., LEHTILA, A., Labriet, M., 2010. TIMES Climate Module (Nov. 2010). TIMES Version 2.0 User Note (November).
- Manne, A., Mendelsohn, R., Richels, R., 1995. MERGE A model for evaluating regional and global effects of GHG reduction policies. *Energy Policy* 23 (1), 17–34.
- Meinshausen, M., Raper, S. C. B., Wigley, T. M. L., 2011. Emulating coupled atmosphere-ocean and carbon cycle models with a simpler model, MAGICC6 - Part 1: Model description and calibration. *Atmospheric Chemistry and Physics* 11, 1417–1456.
- Nordhaus, W., Sztorc, P., 2013. DICE 2013R : Introduction and User ' s Manual with (April), 1–102.

- Nordhaus, W. D., 2008. A Question of Balance: Weighing the Options on Global Warming Policies. Vol. 87.
- Nordhaus, W. D., 2014. Estimates of the social cost of carbon: Concepts and results from the DICE-2013R model and alternative approaches. *Journal of the Association of Environmental and Resource Economists* 1 (1/2), 273–312.
- Nordhaus, W. D., Boyer, J., 1999. *Warming the World*. The MIT Press, Cambridge.
- Pindyck, R. S., 2013. Climate Change Policy : What Do the Models Tell Us ? *Journal of Economic Literature* 51, 860–872.
- Schmidt, H., Alterskjær, K., Alterskjær, K., Bou Karam, D., Boucher, O., Jones, a., Kristjánsson, J. E., Niemeier, U., Schulz, M., Aaheim, a., Benduhn, F., Lawrence, M., Timmreck, C., 2012. Solar irradiance reduction to counteract radiative forcing from a quadrupling of CO<sub>2</sub>: Climate responses simulated by four earth system models. *Earth System Dynamics* 3 (1), 63–78.
- Schneider, S., 1997. Integrated assessment modeling of global climate change: Transparent rational tool for policy making or opaque screen hiding value laden assumptions? *Environmental Modeling and Assessment* 2 (4), 229.
- Smith, M. J., Vanderwel, M. C., Lyutsarev, V., Emmott, S., Purves, D. W., 2012. The climate dependence of the terrestrial carbon cycle; including parameter and structural uncertainties. *Biogeosciences Discussions* 9 (10), 13439–13496.
- Sokolov, A., Schlosser, C., Dutkiewicz, Paltsev, Kicklighter, D., Jacoby, H., Prinn, R., Forest, C., Reilly, J., Wang, C., Felzer, Sarofim, Scott, J., Stone, P., Melillo, J., Cohen, J., 2005. The mit integrated global system model (igsm) version 2: Model description and baseline evaluation. Tech. Rep. 124, MIT Joint Program.
- Soyster, L. A., 1973. Convex Programming with Set-Inclusive Constraints and Applications to Inexact Linear Programming. *Operations Research* 21 (5), 1154–1157.
- Stern, N., 2007. *The Economics of Climate Change: The Stern Review*. Cambridge University Press.
- Stern, N., 2013. The structure of economic modeling of the potential impacts of climate change: Grafting gross underestimation of risk onto already narrow science models. *Journal of Economic Literature* 51 (3), 838–59.
- Stocker, T., Qin, D., Plattner, G.-K., Tignor, M., Allen, S., Boschung, J., Nauels, A., Xia, Y., Bex, V., Midgley, P., 2013. IPCC, 2013: Summary for Policymakers. *Climate Change 2013: The Physical Science Basis*. Contribution of Working Group I to the Fifth Assessment Report of the Intergovernmental Panel on Climate Change.
- Syri, S., Lehtila, A., Ekholm, T., Savolainen, I., Holttinen, H., Peltola, E., Feb. 2008. Global energy and emissions scenarios for effective climate change mitigation—Deterministic and stochastic scenarios with the TIAM model. *International Journal of Greenhouse Gas Control* 2 (2), 274–285.
- United Nations, 2015. Paris agreement to the united nations framework convention on climate change.
- van Asselt, M. B. A., Rotmans, J., 2002. Uncertainty in integrated assessment modelling: From positivism to pluralism. *Climatic Change* 54 (1/2), 75–105.
- van Vuuren, D. P., Lowe, J., Stehfest, E., Gohar, L., Hof, A. F., Hope, C., Warren, R., Meinshausen, M., Plattner, G.-K., Dec. 2009. How well do integrated assessment models simulate climate change? *Climatic Change* 104 (2), 255–285.
- Vanderzwaan, B., Gerlagh, R., nov 2006. Climate sensitivity uncertainty and the necessity to transform global energy supply. *Energy* 31 (14), 2571–2587.

Waisman, H., Guivarch, C., Lecocq, F., 2013. The transportation sector and low-carbon growth pathways: modelling urban, infrastructure, and spatial determinants of mobility. *Climate Policy* 13 (01), 106–129.

Zhang, M., Huang, Y., 2014. Radiative forcing of quadrupling  $\text{CO}_2$ . *Journal of Climate* 27, 2496–2508.

## A. TIAM World Climate Module

The terrestrial carbon cycle of this climate module is depicted in Figure 2. Formally, the one-year-lagged dynamics of the three detailed greenhouse gases are the following:

$$\begin{aligned} \begin{bmatrix} M^{CO_2,a} \\ M^{CO_2,u} \\ M^{CO_2,l} \end{bmatrix}_t &= \Phi^{CO_2} \begin{bmatrix} M^{CO_2,a} \\ M^{CO_2,u} \\ M^{CO_2,l} \end{bmatrix}_{t-1} + \begin{bmatrix} 1 \\ 0 \\ 0 \end{bmatrix} E_t^{CO_2}, \\ \begin{bmatrix} M^{CH_4,a} \\ M^{CH_4,u} \end{bmatrix}_t &= \Phi^{CH_4} \begin{bmatrix} M^{CH_4,a} \\ M^{CH_4,u} \end{bmatrix}_{t-1} + \begin{bmatrix} 1 \\ 0 \end{bmatrix} E_t^{CH_4}, \\ \begin{bmatrix} M^{N_2O,a} \\ M^{N_2O,u} \end{bmatrix}_t &= \Phi^{N_2O} \begin{bmatrix} M^{N_2O,a} \\ M^{N_2O,u} \end{bmatrix}_{t-1} + \begin{bmatrix} 1 \\ 0 \end{bmatrix} E_t^{N_2O}, \\ \Phi^{CO_2} &= \begin{bmatrix} 1 - \varphi^{a-u} & \varphi^{u-a} & 0 \\ \varphi^{a-u} & 1 - \varphi^{u-a} - \varphi^{u-l} & \varphi^{l-u} \\ 0 & \varphi^{u-l} & 1 - \varphi^{l-u} \end{bmatrix}, \\ \Phi^{CH_4} &= \begin{bmatrix} \varphi^{CH_4} & 0 \\ 0 & 1 \end{bmatrix}, \Phi^{N_2O} = \begin{bmatrix} \varphi^{N_2O} & 0 \\ 0 & 1 \end{bmatrix}, \end{aligned}$$

where  $M_t^{g,r}$  is the mass of gas  $g$  in reservoir  $r$  in year  $t$ ,  $E_t^g$  is the emission of gas  $g$  in year  $t$  (from the global energy model),  $\varphi^{r_o,r_i}$  is the transfer coefficient for  $CO_2$  from reservoir  $r_o$  to reservoir  $r_i$ ,  $\varphi^{CH_4}$  and  $\varphi^{N_2O}$  are the decay rates of methane and nitrous oxide in the atmosphere,  $g \in G = \{CO_2, CH_4, N_2O\}$  and  $r \in R = \{a = \text{Atmosphere}, u = \text{UpperLayer}, l = \text{LowerLayer}\}$ .

This set of equations defining the time profiles of atmospheric GHGs is then used to compute the radiative forcing. It is common (IPCC, 2007) to consider that forcings are additive, so that:

$$\Delta F_t = \sum_{g \in G} \Delta F_t^g + Exf_t,$$

where  $\Delta F_t^g$  is the forcing of gas  $g$  in period  $t$  and  $Exf_t$  corresponds to an exogenous assumption of forcing for all gases other than carbon dioxide, methane and nitrous oxide. The current knowledge on radiative forcing suggests that none of these terms is linear in the atmospheric stock of gas; the linearization used here is proposed by Loulou et al. (2010):

$$\begin{aligned} \Delta F_t^{CO_2} &= \gamma A^{CO_2} + \gamma B^{CO_2} M_t^{CO_2,a}, \\ \Delta F_t^{CH_4} &= A^{CH_4} + B^{CH_4} M_t^{CH_4,a}, \\ \Delta F_t^{N_2O} &= A^{N_2O} + B^{N_2O} M_t^{N_2O,a}, \end{aligned}$$

where  $\gamma$  is the radiative forcing sensitivity to atmospheric  $CO_2$  doubling, and  $A$ 's and  $B$ 's are constant depending on pre-industrial concentration levels and linearization intervals. Finally, temperature elevation profiles are computed based on the following equations:

$$\begin{aligned} \begin{bmatrix} \Delta T^{up} \\ \Delta T^{lo} \end{bmatrix}_t &= S \begin{bmatrix} \Delta T^{up} \\ \Delta T^{lo} \end{bmatrix}_{t-1} + \begin{bmatrix} \sigma_1 \\ 0 \end{bmatrix} \Delta F_t, \\ S &= \begin{bmatrix} 1 - \sigma_1 \left( \frac{\gamma}{C_S} + \sigma_2 \right) & \sigma_1 \sigma_2 \\ \sigma_3 & 1 - \sigma_3 \end{bmatrix}. \end{aligned}$$

where  $\Delta T^{up}$  is the variation of the atmospheric temperature,  $\Delta T^{lo}$  the variation of the ocean temperature,  $C_S$  represents the climate sensitivity, i.e. the change in equilibrium atmospheric temperature due to a doubling of GHG concentration;  $\sigma_1$  and  $\sigma_3$  are the adjustment speeds for respectively atmospheric and oceanic temperature (lags, in  $year^{-1}$ );  $\sigma_2$  is a heat loss coefficient from the atmosphere to the deep ocean.

## B. Estimation of lower/upper bounds for climate parameters

Overall, and in the course of this estimation exercise, we may classify the climate parameters at stake in this study into three groups. First, *one group contains the parameters for the carbon cycle*. The terrestrial carbon cycle itself is a rather large field of study in geophysics (see e.g. [Smith et al., 2012](#); [Joos et al., 2013](#); for a multi-model approach). One can also find sensitivity analysis on the carbon cycle in IAM-based research ([Butler et al., 2014](#); [Hof et al., 2012](#)), or are least clues on how uncertain these parameters are ([Nordhaus, 2008](#)). One way of assessing the behavior of carbon cycle models is to perform the so-called ‘doubling experiment’, where the evolution of an atmospheric CO<sub>2</sub> doubling-concentration pulse in year 0 is followed across the various carbon sinks for the next 100-400 years. Existing multi-models experiments ([Joos et al., 2013](#); [van Vuuren et al., 2009](#)) point out large response spectra; [van Vuuren et al. \(2009\)](#) additionally show that simple carbon models (few boxes, simple linear recursive dynamics) such as DICE end up in the low range of possible outcomes: they have, compared to the rest, relatively optimistic carbon cycles. Such an experiment seems to be a good starting point to calibrate a carbon cycle. However, the uncertainty it translates covers both parametric and structural uncertainty. For example, [van Vuuren et al. \(2009\)](#) argue that the PAGE model behaves very differently from the rest of the test population because it includes feedbacks on the carbon cycle. This limitation – carbon cycle models have different structures, hence different parameters – makes it difficult to adopt such a calibration procedure. Therefore, we adopt a calibration procedure similar to that of [Nordhaus and Sztorc \(2013\)](#), but for the four IPCC-RCP emissions scenarios ran under the multi-ensemble simulation mode of MAGICC6 ([Meinshausen et al., 2011](#)). To this purpose:

- the nominal values of the parameters in the climate module in TIAM-World was left as described in [Loulou et al. \(2010\)](#);
- the upper bound of the inter-boxes transfer coefficients were estimated to get close to the 83rd percentile of the MAGICC6 inter-model simulations for the four RCP scenarios. This is done by changing the parameters by identical relative amounts, and computing a simple distance measure (the sum of squares of annual relative distances between the TIAM-climate simulation and the MAGICC6-RCP benchmark).

The result of this experiment is shown in Figure 12. The blue lines and shade represent, in each subgraph, the average, 95% and 90% confidence intervals produced by MAGICC6. The black plain and dotted show the average and 95% confidence intervals obtained with the TIAM-World climate module.

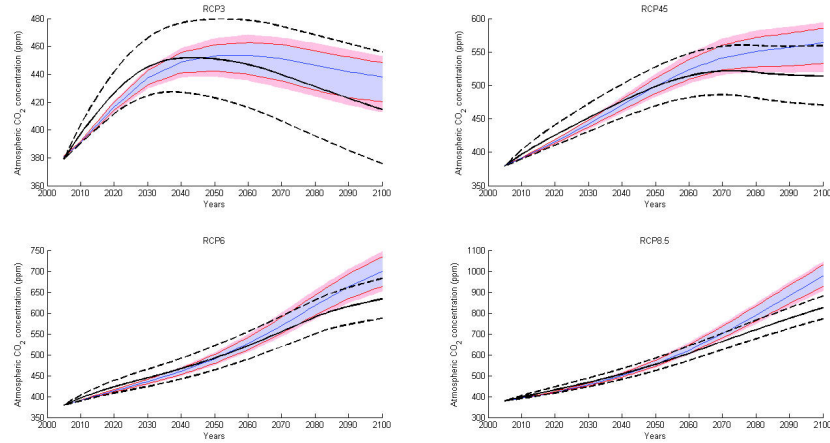


**Figure 12:** TIAM-World climate module: Uncertainty in the carbon cycle against MAGICC6 ranges for the four RCP scenarios

These variations allow to capture only a minor part of the carbon cycle model variations described by Joos et al. (2013) or van Vuuren et al. (2009). Hof et al. (2012) show that the variations in climate change benefits from a set of IAMs due to the carbon cycle are lower than the MAGICC6 ranges, which seems to indeed indicate that simple carbon cycles do not capture all the ‘volatility’ of outcomes.

A second set of parameters includes the forcing and climate sensitivities, which are likely to be the most well-documented parameters in the climate literature. They traduce the global equilibrium surface forcing and warming after a doubling of atmospheric CO<sub>2</sub> concentration; any climate models includes these parameters. The importance of the equilibrium radiative forcing is widely acknowledged (Cao et al., 2010); multi-models comparisons and simulations are also frequent (Schmidt et al., 2012). If issues such as climate feedbacks arise in the estimation of forcing (Block and Mauritsen, 2013), available comparisons indicate plausible range for the forcing parameters (using doubling or quadrupling experiments), with the last IPCC report (AR5-WG1, Stocker et al., 2013) providing a central value of 3.7 with a +/- 0.8 99% confidence interval. This estimation is consistent with Zhang and Huang (2014), and is retained for this study. As for the climate sensitivity, the initial value of the TIAM-World calibration corresponds to the Knutti and Hegerl (2008) synthesize plausible sensitivity ranges for the climate sensitivity for different lines of evidence, and demonstrate how critical it is if the policy objective is to prevent damages caused by certain levels of warming. The IPCC most likely value and upper bound are 3 °C and 4.5 °C respectively, which is consistent with other papers such as Syri et al. (2008). Butler et al. (2014) make a different choice, and end up with a range (upper bound of 8 °C) closer to what Knutti and Hegerl (2008) refer to as ‘expert elicitation’. Combining different lines of evidence, these authors obtain a range close to the one of IPCC, which we will retain as a basis. Compared to existing literature on IAM-SCM sensitivity analysis in Butler et al. (2014), these ranges are high for forcing and low for the climate sensitivity.

Finally, the rest of the parameters, traducing the temperature dynamics, are part of a third group constituted of apparently less studied parameters. There seems to be considerably less available work on these. By default, we proceed as Butler et al. (2014), and apply a 10% variation to the annual heat transfer coefficients. The range of temperature responses of TIAM-World are compared against MAGICC6 for the 4 RCPs scenarios, accounting for the uncertainty of all parameters. The results are presented in Figure 13 (it reads as Figure 12).

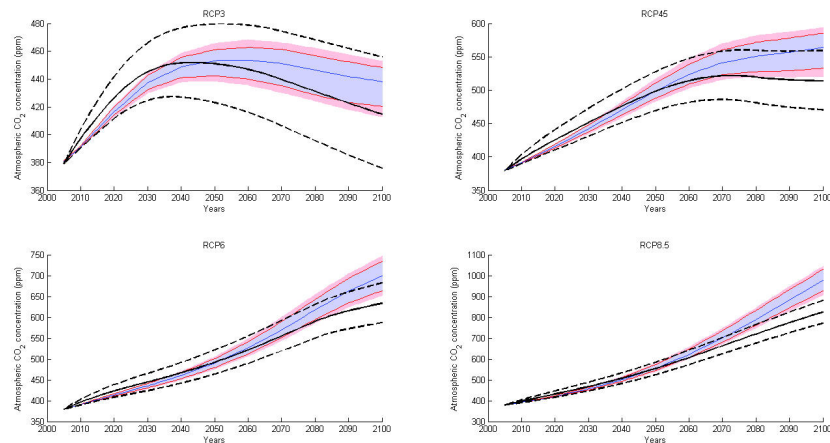


**Figure 13:** TIAM-World climate module: Uncertainty in the global mean temperature against MAGICC6 ranges for the four RCP scenarios

The final nominal values and ranges for the climate parameters are presented in Figure 3 along with the values kept in Butler et al. (2014) for comparison purposes.

| Parameter    | Description                                                    | Nominal value | Lower/Upper bound | Nominal value (Butler et al., 2014) | Lower/Upper bound (Butler et al., 2014) |
|--------------|----------------------------------------------------------------|---------------|-------------------|-------------------------------------|-----------------------------------------|
| $\phi_{a-u}$ | Atmosphere to upper layer carbon transfer coefficient (annual) | 0.046         | 0.04393           | 0.189288                            | 0.223288                                |
| $\phi_{u-a}$ | Upper layer to atmosphere carbon transfer coefficient (annual) | 0.0453        | 0.0473385         | 0.097213                            | derived                                 |
| $\phi_{u-l}$ | Upper to lower layer carbon transfer coefficient (annual)      | 0.0146        | 0.013943          | 0.05                                | 0.025                                   |
| $\phi_{l-u}$ | Lower to upper layer carbon transfer coefficient (annual)      | 0.00053       | 0.00055385        | 0.003119                            | derived                                 |
| $\gamma$     | Radiative forcing from doubling of CO <sub>2</sub>             | 3.7           | 4.5               | 3.8                                 | 3.9                                     |
| $C_S$        | Climate sensitivity from doubling of CO <sub>2</sub>           | 2.9           | 4.5               | 3                                   | 8                                       |
| $\sigma_1$   | Adjustment speed of atmospheric temperature                    | 0.024         | 0.0264            | 0.22                                | 0.24                                    |
| $\sigma_2$   | Heat loss from atmosphere to deep ocean                        | 0.44          | 0.396             | 0.3                                 | 0.27                                    |
| $\sigma_3$   | Heat gain by deep ocean                                        | 0.002         | 0.0018            | 0.05                                | 0.045                                   |

**Table 3:** Nominal values for climate parameters and comparison with Butler et al. (2014)

### C. Appendix : Implementation details for the worst-case oracle in TIAM-World model

For simplicity of exposure, we describe the procedure for solving Problem (14) when the respective worst-case extreme value (between minimum and maximum) for each parameter can be identified a-priori (either analytically or using common sense). Following the information presented in Table 1, we can describe the uncertainty as follows:

$$\begin{aligned}
\psi^{a-u} &:= \bar{\psi}^{a-u} - \hat{\psi}^{a-u} z_1 & \psi^{u-a} &:= \bar{\psi}^{u-a} + \hat{\psi}^{u-a} z_2 \\
\psi^{u-l} &:= \bar{\psi}^{u-l} - \hat{\psi}^{u-l} z_3 & \psi^{l-u} &:= \bar{\psi}^{l-u} + \hat{\psi}^{l-u} z_4 \\
\gamma &:= \bar{\gamma} + \hat{\gamma} z_5 & (1/C_s) &:= (1/\bar{C}_s) - (\hat{C}_s/(\bar{C}_s^2 + \bar{C}_s \hat{C}_s)) z_6 \\
\sigma_1 &:= \bar{\sigma}_1 + \hat{\sigma}_1 z_7 & \sigma_2 &:= \bar{\sigma}_2 + \hat{\sigma}_2 z_8 \\
\sigma_3 &:= \bar{\sigma}_3 + \hat{\sigma}_3 z_9,
\end{aligned}$$

where the “bar” annotated parameter refers to the nominal value and the “hat” annotated parameter refers to the magnitude of the perturbation needed to get to the chosen extreme value. We also modeled the perturbation on the term  $1/C_s$  using an additive formulation, namely:

$$1/C_s := \begin{cases} 1/\bar{C}_s & \text{if } z_6 = 1 \\ 1/(\bar{C}_s + \hat{C}_s) & \text{otherwise} \end{cases} .$$

Based on the definitions of  $A$  and  $F$ , one should notice that these two matrices are not linear functions of the uncertainty  $z_1, z_2, \dots, z_9$ . This can be remedied by replacing the nonlinearities with additional binary variables. In particular, when studying the effect of  $z$  on each term of  $A$ , one might realize that the following expressions come into play:

$$\left\{ \begin{array}{l} \gamma\psi^{a-u} = \bar{\gamma}\bar{\psi}^{a-u} - \bar{\gamma}\hat{\psi}^{a-u}z_1 + \bar{\psi}^{a-u}\hat{\gamma}z_5 - \hat{\gamma}\hat{\psi}^{a-u}z_1z_5 \\ \gamma\psi^{u-a} = \bar{\gamma}\bar{\psi}^{u-a} + \bar{\gamma}\hat{\psi}^{u-a}z_2 + \bar{\psi}^{u-a}\hat{\gamma}z_5 + \hat{\gamma}\hat{\psi}^{u-a}z_2z_5 \\ \sigma_1\gamma\psi^{a-u} = \bar{\sigma}_1\bar{\gamma}\bar{\psi}^{a-u} - \bar{\sigma}_1\bar{\gamma}\hat{\psi}^{a-u}z_1 + \bar{\sigma}_1\hat{\gamma}\bar{\psi}^{a-u}z_5 + \hat{\sigma}_1\bar{\gamma}\bar{\psi}^{a-u}z_7 \\ \quad - \bar{\sigma}_1\hat{\gamma}\hat{\psi}^{a-u}z_1z_5 - \hat{\sigma}_1\bar{\gamma}\hat{\psi}^{a-u}z_1z_7 + \hat{\sigma}_1\hat{\gamma}\bar{\psi}^{a-u}z_5z_7 + \hat{\sigma}_1\hat{\gamma}\hat{\psi}^{a-u}z_1z_5z_7 \\ \sigma_1\gamma\psi^{u-a} = \bar{\sigma}_1\bar{\gamma}\bar{\psi}^{u-a} + \bar{\sigma}_1\bar{\gamma}\hat{\psi}^{u-a}z_2 + \bar{\sigma}_1\hat{\gamma}\bar{\psi}^{u-a}z_5 + \hat{\sigma}_1\bar{\gamma}\bar{\psi}^{u-a}z_7 \\ \quad + \bar{\sigma}_1\hat{\gamma}\hat{\psi}^{u-a}z_2z_5 + \hat{\sigma}_1\bar{\gamma}\hat{\psi}^{u-a}z_2z_7 + \hat{\sigma}_1\hat{\gamma}\bar{\psi}^{u-a}z_5z_7 + \hat{\sigma}_1\hat{\gamma}\hat{\psi}^{u-a}z_2z_5z_7 \\ \sigma_1\gamma/C_s = \bar{\sigma}_1\bar{\gamma}\bar{\theta} + \bar{\sigma}_1\hat{\gamma}\hat{\theta}z_5 - \bar{\sigma}_1\hat{\gamma}\hat{\theta}z_6 + \hat{\sigma}_1\bar{\gamma}\bar{\theta}z_7 \\ \quad - \bar{\sigma}_1\hat{\gamma}\hat{\theta}z_5z_6 + \hat{\sigma}_1\hat{\gamma}\bar{\theta}z_5z_7 - \hat{\sigma}_1\hat{\gamma}\hat{\theta}z_6z_7 - \hat{\sigma}_1\hat{\gamma}\hat{\theta}z_5z_6z_7 \\ \sigma_1\sigma_2 = \bar{\sigma}_1\bar{\sigma}_1 + \hat{\sigma}_1\bar{\sigma}_1z_7 + \bar{\sigma}_1\hat{\sigma}_2z_8 + \bar{\sigma}_1\hat{\sigma}_2z_7z_8, \end{array} \right.$$

where  $\bar{\theta} := 1/\bar{C}_s$  and  $\hat{\theta} := \hat{C}_s/(\bar{C}_s^2 + \bar{C}_s\hat{C}_s)$ . By making the replacement  $v_{0jk} := z_jz_k$  and  $v_{ijk} := z_iz_jz_k$ , one would instead get the following set of linear representations:

$$\left\{ \begin{array}{l} \gamma\psi^{a-u} = \bar{\gamma}\bar{\psi}^{a-u} - \bar{\gamma}\hat{\psi}^{a-u}z_1 + \bar{\psi}^{a-u}\hat{\gamma}z_5 - \hat{\gamma}\hat{\psi}^{a-u}v_{015} \\ \gamma\psi^{u-a} = \bar{\gamma}\bar{\psi}^{u-a} + \bar{\gamma}\hat{\psi}^{u-a}z_2 + \bar{\psi}^{u-a}\hat{\gamma}z_5 + \hat{\gamma}\hat{\psi}^{u-a}v_{025} \\ \sigma_1\gamma\psi^{a-u} = \bar{\sigma}_1\bar{\gamma}\bar{\psi}^{a-u} - \bar{\sigma}_1\bar{\gamma}\hat{\psi}^{a-u}z_1 + \bar{\sigma}_1\hat{\gamma}\bar{\psi}^{a-u}z_5 + \hat{\sigma}_1\bar{\gamma}\bar{\psi}^{a-u}z_7 \\ \quad - \bar{\sigma}_1\hat{\gamma}\hat{\psi}^{a-u}v_{015} - \hat{\sigma}_1\bar{\gamma}\hat{\psi}^{a-u}v_{017} + \hat{\sigma}_1\hat{\gamma}\bar{\psi}^{a-u}v_{057} + \hat{\sigma}_1\hat{\gamma}\hat{\psi}^{a-u}v_{157} \\ \sigma_1\gamma\psi^{u-a} = \bar{\sigma}_1\bar{\gamma}\bar{\psi}^{u-a} + \bar{\sigma}_1\bar{\gamma}\hat{\psi}^{u-a}z_2 + \bar{\sigma}_1\hat{\gamma}\bar{\psi}^{u-a}z_5 + \hat{\sigma}_1\bar{\gamma}\bar{\psi}^{u-a}z_7 \\ \quad + \bar{\sigma}_1\hat{\gamma}\hat{\psi}^{u-a}v_{025} + \hat{\sigma}_1\bar{\gamma}\hat{\psi}^{u-a}v_{027} + \hat{\sigma}_1\hat{\gamma}\bar{\psi}^{u-a}v_{057} + \hat{\sigma}_1\hat{\gamma}\hat{\psi}^{u-a}v_{257} \\ \sigma_1\gamma/C_s = \bar{\sigma}_1\bar{\gamma}\bar{\theta} + \bar{\sigma}_1\hat{\gamma}\hat{\theta}z_5 - \bar{\sigma}_1\hat{\gamma}\hat{\theta}z_6 + \hat{\sigma}_1\bar{\gamma}\bar{\theta}z_7 \\ \quad - \bar{\sigma}_1\hat{\gamma}\hat{\theta}v_{056} + \hat{\sigma}_1\hat{\gamma}\bar{\theta}v_{057} - \hat{\sigma}_1\hat{\gamma}\hat{\theta}v_{067} - \hat{\sigma}_1\hat{\gamma}\hat{\theta}v_{567} \\ \sigma_1\sigma_2 = \bar{\sigma}_1\bar{\sigma}_1 + \hat{\sigma}_1\bar{\sigma}_1z_7 + \bar{\sigma}_1\hat{\sigma}_2z_8 + \bar{\sigma}_1\hat{\sigma}_2v_{078}, \end{array} \right.$$

Hence it becomes possible to represent  $\mathbb{U}$  as:

$$\mathbb{U} := \left\{ (A, F) \in \mathbb{R}^{w \times w} \times \mathbb{R}^{w \times n} \left| \begin{array}{l} \exists z_0 = 1, z \in \{0, 1\}^m, v \in \{0, 1\}^{|\mathcal{S}|} \\ \sum_{i=1}^m z_i \leq \Gamma \\ A = \bar{A} + \sum_{i=1}^m \hat{A}_i z_i + \sum_{(i,j,k) \in \mathcal{S}} \tilde{A}_{ijk} v_{ijk} \\ F = \bar{F} + \sum_{i=1}^m \hat{F}_i z_i + \sum_{(i,j,k) \in \mathcal{S}} \tilde{F}_{ijk} v_{ijk} \\ z_i + z_j + z_k - 2 \leq v_{ijk} \leq (1/3)(z_i + z_j + z_k), \forall (i, j, k) \in \mathcal{S} \end{array} \right. \right\}$$

where

$$\mathcal{S} := \{(0, 1, 5), (0, 1, 7), (0, 2, 5), (0, 2, 7), (0, 5, 6), (0, 5, 7), (0, 6, 7), (0, 7, 8), (1, 5, 7), (2, 5, 7), (5, 6, 7)\},$$

and where  $\bar{A} + \sum_i \hat{A}_i z_i + \sum_{(i,j,k) \in \mathcal{S}} \tilde{A}_{ijk} v_{ijk}$  and  $\bar{F} + \sum_i \hat{F}_i z_i + \sum_{(i,j,k) \in \mathcal{S}} \tilde{F}_{ijk} v_{ijk}$  are the respective linear matrix representations of  $A$  and  $F$ . Furthermore, the set of linear constraints that take the form:

$$z_i + z_j + z_k - 2 \leq v_{ijk} \leq (1/3)(z_i + z_j + z_k),$$

are simply a convenient way of representing the nonlinear equality constraint  $v_{ijk} = z_iz_jz_k$ .



Having this representation for  $\mathbb{U}$  in hand, Problem (14) can be described as:

$$\left\{ \begin{array}{l} \max_{y,z,v} y_t - w_t \\ \text{s.t. } y_{\tau+1} = (\bar{A} + \sum_i \hat{A}_i z_i + \sum_{(i,j,k) \in \mathcal{S}} \tilde{A}_{ijk} v_{ijk}) y_\tau \\ \quad + (\bar{F} + \sum_i \hat{F}_i z_i + \sum_{(i,j,k) \in \mathcal{S}} \tilde{F}_{ijk} v_{ijk}) x_\tau, \forall \tau = 1, \dots, t \\ \sum_i z_i \leq \Gamma \\ z_i + z_j + z_k - 2 \leq v_{ijk} \leq (1/3)(z_i + z_j + z_k), \forall (i,j,k) \in \mathcal{S} \\ z \in \{0,1\}^m, v \in \{0,1\}^{|\mathcal{S}|} \end{array} \right.$$

which is still a mixed integer nonlinear program due to the cross-terms  $z_i y_\tau$  and  $v_{ijk} y_\tau$ .

In order to facilitate the resolution, we apply a second step of linearization by employing additional variables  $Z \in \mathbb{R}^{m \times t}$  and  $V \in \mathbb{R}^{|\mathcal{S}| \times t}$  such that  $Z_{i,\tau} := z_i y_\tau$  and  $V_{ijk,\tau} := v_{ijk} y_\tau$ . This leads to the following mixed integer linear program:

$$\left\{ \begin{array}{l} \max_{y,z,v,Z,V} y_t \\ \text{s.t. } y_{\tau+1} = \bar{A} y_\tau + \sum_i \hat{A}_i Z_{i,\tau} + \sum_{(i,j,k) \in \mathcal{S}} \tilde{A}_{ijk} V_{ijk,\tau} + \bar{F} x_\tau + \sum_i \hat{F}_i x_\tau z_i + \sum_{(i,j,k) \in \mathcal{S}} \tilde{F}_{ijk} x_\tau v_{ijk} \\ \quad \bar{F} x_\tau + \sum_i \hat{F}_i x_\tau z_i + \sum_{(i,j,k) \in \mathcal{S}} \tilde{F}_{ijk} x_\tau v_{ijk} \\ -M_1 z_i \leq Z_{i,\tau} \leq M_2 z_i \\ y_\tau - M_2(1-z_i) \leq Z_{i,\tau} \leq y_\tau + M_1(1-z_i) \\ -M_1 v_i \leq V_{i,\tau} \leq M_2 v_i \\ y_\tau - M_2(1-v_i) \leq V_{i,\tau} \leq y_\tau + M_1(1-v_i) \\ \sum_i z_i \leq \Gamma \\ z_i + z_j + z_k - 2 \leq v_{ijk} \leq (1/3)(z_i + z_j + z_k), \forall (i,j,k) \in \mathcal{S} \\ z \in \{0,1\}^m, v \in \{0,1\}^{|\mathcal{S}|}, \end{array} \right.$$

where  $M_1$  and  $M_2$  are large enough constants that are known to capture  $-M_1 \leq y_\tau^* \leq M_2$ . One can easily verify that the ‘‘big M’’ constraints on  $Z_{i,\tau}$  and  $V_{ijk,\tau}$  are equivalent to imposing that  $Z_{i,\tau} := z_i y_\tau$  and  $V_{ijk,\tau} := v_{ijk} y_\tau$ .

## D. Monte-Carlo simulations of the temperature

For readability reasons, we plot only 100 trajectories (to calculate the CVaR, we have realized 2,000 draws).

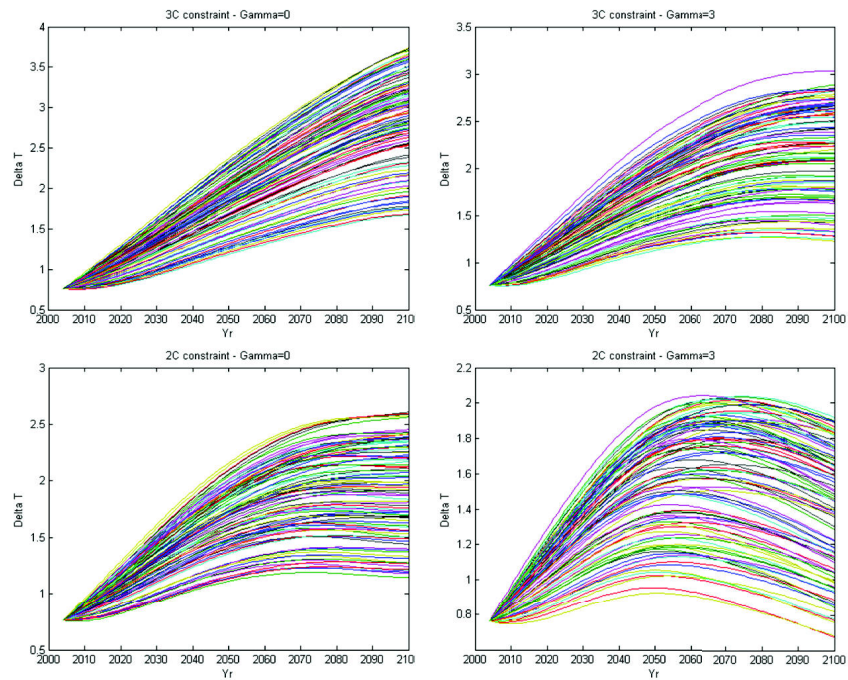


**Figure 14:** Temperature trajectories (2 °C and 3 °C emission pathways with  $\Gamma = 0$  and  $\Gamma = 3$ )

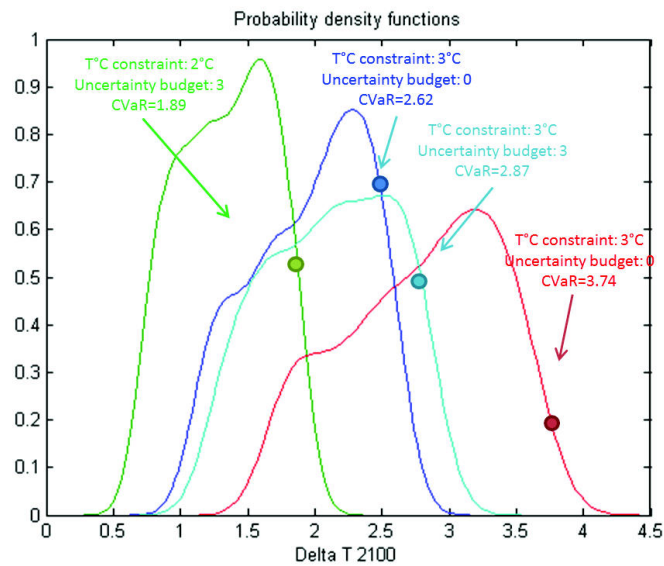


**Figure 15:** 2100 Temperature delta (2 °C and 3 °C emission pathways with  $\Gamma = 0$  and  $\Gamma = 3$ ) – Density functions and CVaR

# The "*Cahiers de l'Économie*" Series

The "*Cahiers de l'Économie*" Series of occasional discussion papers was launched in 1990 with the aim to enable scholars, researchers and practitioners to share important ideas with a broad audience of stakeholders including, academics, government departments, regulators, policy organisations and energy companies.

All these discussion papers are available upon request at IFP School. Discussion papers from 2004 onwards can be downloaded at: [www.ifpen.fr](http://www.ifpen.fr)

The list of discussion papers from 2006 onwards includes:

**# 59. F. LESCAROUX**

The Economic Consequences of Rising Oil Prices.  
Mai 2006

**# 60. F. LESCAROUX, O. RECH**

L'origine des disparités de demande de carburant dans l'espace et le temps : l'effet de la saturation de l'équipement en automobiles sur l'élasticité revenu.  
Juin 2006

**# 61. C. I. VASQUEZ JOSSE, A. NEUMANN**

Transatlantic Natural Gas Price and Oil Price Relationships - An Empirical Analysis.  
Septembre 2006

**# 62. E. HACHE**

Une analyse de la stratégie des compagnies pétrolières internationales entre 1999 et 2004.  
Juillet 2006

**# 63. F. BERNARD, A. PRIEUR**

Biofuel market and carbon modelling to evaluate French biofuel policy.  
Octobre 2006

**# 64. E. HACHE**

Que font les compagnies pétrolières internationales de leurs profits ?  
Janvier 2007

**# 65. A. PIERRU**

A note on the valuation of subsidized Loans  
Janvier 2007

**# 66. D. BABUSIAUX, P. R. BAUQUIS**

Depletion of Petroleum Reserves and Oil Price trends  
Septembre 2007

**# 67. F. LESCAROUX**

Car ownership in relation to income distribution and consumers's spending decisions.  
Novembre 2007

**# 68. D. BABUSIAUX, A. PIERRU**

Short-run and long-run marginal costs of joint products in linear programming  
Juin 2008

**# 69. E. HACHE**

Commodities Markets: New paradigm or new fashion?  
Juillet 2008

**# 70. D. BABUSIAUX, A. PIERRU**

Investment project valuation: A new equity perspective  
Février 2009

**# 71. O. MASSOL, S. TCHUNG-MING**

Stratégies coopératives dans l'industrie du GNL : l'argument de la rationalisation est-il fondé ?  
Février 2009

**# 72. A. PIERRU, D. BABUSIAUX**

Valuation of investment projects by an international oil company: A new proof of a straightforward, rigorous method

Février 2009

**# 73. E. SENTENAC CHEMIN**

Is the price effect on fuel consumption symmetric? Some evidence from an empirical study  
Avril 2009

**# 74. E. HACHE**

OBAMA : Vers un green New Deal énergétique ?  
Septembre 2009

**# 75. O. MASSOL**

Cost function for the natural gas transmission industry: further considerations  
Septembre 2009

**# 76. F. LANTZ, E. SENTENAC CHEMIN**

Analyse des tendances et des ruptures sur le marché automobile français. Modélisation du taux de diésélisation dans le parc  
Décembre 2010.

**# 77. B. CHÈZE, P. GASTINEAU, J. CHEVALLIER**

Forecasting air traffic and corresponding Jet-Fuel Demand until 2025  
Décembre 2010.

**# 78. V. BREMOND, E. HACHE, V. MIGNON**

Does OPEC still exist as a cartel? An empirical investigation  
Mars 2011.

**# 79. I. ABADA, O. MASSOL**

Security of supply and retail competition in the European gas market. Some model-based insights.  
Mars 2011.

**# 80. E. HACHE, F. LANTZ**

Oil price volatility: an econometric analysis of the WTI market.  
Avril 2011.

**# 81. I. ABADA, V. BRIAT, O. MASSOL**

Construction of a fuel demand function portraying interfuel substitution, a system dynamics approach.  
Avril 2011

**# 82. E. LE CADRE, F. LANTZ, P-A. JOUVET**

The bioenergies development: the role of biofuels and the CO2 price.  
Décembre 2011

**# 83. E. LE CADRE, F. LANTZ, A. FARNOOSH**

Bioenergies usages in electricity generation utility means through a modelling approach: application to the French case.  
Décembre 2011

**# 84. I. ABADA, V. BRIAT, S. GABRIEL, O. MASSOL**

A generalized Nash-Cournot model for the north-western European natural gas markets with a fuel substitution demand function: the GaMMES model.  
Décembre 2011

**# 85. O. MASSOL, A. BANAL-ESTAÑOL**

Export diversification and resource-based industrialization: the case of natural gas.  
Décembre 2011

**# 86. B. CHÈZE, P. GASTINEAU, J. CHEVALLIER**

Air traffic energy efficiency differs from place to place: analysis of historical trends by geographical zones using a macro-level methodology.

Décembre 2011

**# 87. D. LORNE, S. TCHUNG-MING**

The French biofuels mandates under cost uncertainty – an assessment based on robust optimization.

Septembre 2012

**# 88. L. de MAACK, F. LANTZ**

Petroleum products price interactions on the world markets: an econometric analysis.

Septembre 2012

**# 89. O. MASSOL, S. TCHUNG-MING**

Joining the CCS Club! Insights from a Northwest European CO<sub>2</sub> Pipeline Project.

Octobre 2012

**# 90. F.M. MENTEN, S. TCHUNG-MING, D. LORNE, F. BOUVART**

Lessons from the use of a long-term energy model for consequential life cycle assessment: the BTL case.

Novembre 2013

**# 91. A. CHEVALIER, F. LANTZ**

Personal car or shared car? Predicting potential modal shifts from multinomial logit models and bootstrap confidence intervals

Novembre 2013

**# 92. A. FARNOOSH, F. LANTZ, J. PERCEBOIS**

Electricity generation analyses in an oil-exporting country: Transition to non-fossil fuel based power units in Saudi Arabia

Décembre 2013

**# 93. V. BREMOND, E. HACHE, M. JOËTS**

On the link between oil and commodity prices: a panel VAR approach.

Décembre 2013

**# 94. B. CHÈZE, J. CHEVALLIER, P. GASTINEAU**

Will technological progress be sufficient to stabilize CO<sub>2</sub> emissions from air transport in the mid-term?

Décembre 2013

**# 95. F. MENTEN, B. CHÈZE, L. PATOULLARD, F. BOUVART**

The use of Meta-Regression Analysis to harmonize LCA literature: an application to GHG emissions of 2<sup>nd</sup> and 3<sup>rd</sup> generation biofuels

Décembre 2013

**# 96. A. DIAZ, S. PROOST**

Second-best urban tolling with distributive concerns.

Décembre 2013

**# 97. O. MASSOL, A. BANAL-ESTAÑOL**

Market power across the Channel: Are Continental European gas markets isolated?

Janvier 2014

**# 98. C. NICOLAS, V. SAINT-ANTONIN, S. TCHUNG-MING**

(How) does sectoral detail affect the robustness of policy insights from energy system models? The refining sector's example

Octobre 2014

**# 99. V. BREMOND, E. HACHE, T. RAZAFINDRABE**

On the link between oil price and exchange rate: A time-varying VAR parameter approach.

Juillet 2015

**# 100. A. BANAL-ESTAÑOL, J. ECKHAUSE, O. MASSOL**

Incentives for early adoption of carbon capture technology: further considerations from a European perspective.

Juillet 2015

**# 101. A. FARNOOSH, F. LANTZ**

Decarbonisation of electricity generation in an oil & gas producing country: "A sensitivity analysis over the power sector in Egypt"

Juillet 2015

**# 102. F. FOSSE, E. HACHE, P. PORTENART**

Un nouveau cycle de fusions et acquisitions dans le secteur des hydrocarbures ? Une analyse économique et historique de la période 2008-2015

Avril 2016

**# 103. E. HACHE, D. LEBoulLENGER, V. MIGNON**

Beyond average energy consumption in the French residential housing market: A household classification approach

Avril 2016

**# 104. A. PARIS**

The Effect of Biofuels on the Link between Oil and Agricultural Commodity Prices: A Smooth Transition Cointegration Approach.

Avril 2016

**# 105. A. FARNOOSH**

On the economic optimization of national power generation mix in Iran: A Markowitz' portfolio-based approach.

Avril 2016

**# 106. E. HACHE, O. MASSOL**

Sanctions against Iran: An assessment of their global impact through the lens of international methanol prices.

Avril 2016

**# 107. M. DUPOUX**

The land use change time-accounting failure.

Juillet 2016

**# 108. C. NICOLAS, S. TCHUNG-MING, O. BAHN, E. DELAGE**

Robust Energy Transition Pathways for Global Warming Targets

Septembre 2016